Annu. Rev. Pharmacol. Toxicol. 1994. 34:281–320

THE CHOLINESTERASES: FROM GENES TO PROTEINS

Palmer Taylor and Zoran Radić[1]
Department of Pharmacology, University of California, San Diego, La Jolla, California 92093

KEY WORDS: acetylcholinesterase, butyrylcholinesterase, alternative mRNA processing, serine hydrolase, site-specific mutagenesis

INTRODUCTION

Linkages between cholinesterases and the pharmacological sciences extend back to the mid-nineteenth century when the first organophosphate was synthesized (1) and physostigmine was recognized in the western world for possessing pharmacological activity (2). However, not until Sir Henry Dale (3) delineated two components of the cholinergic nervous system was the suggestion made that physostigmine inhibited an enzyme that catalyzed the breakdown of choline esters. Dale's and later Loewi & Navratil's (4) studies established a role for acetylcholine as a labile neurotransmitter. The high turnover number of acetylcholinesterase (AChE), the specificity of its inhibitors, and the selectivity of thiocholine-metal ion interactions provided the bases for sensitive in vitro and in situ assay systems (5–7). Several cholinesterase inhibitors remain of value as medicinal agents and insecticides, but others possess the potential for insidious use as chemical warfare agents (8).

Despite this long history of study, less than a decade has passed since the primary structure of a cholinesterase was determined (9), and only in 1991 was its crystal structure solved (10). Clearly, these recent events have added a new perspective to cholinesterase research wherein all facets of gene expression become amenable to study and structure-function relationships within this family of enzymes can be approached at an atomic level

[1]Visiting Fellow from Institute for Medical Research and Occupational Health, University of Zagreb, Croatia

0362-1642/94/0415-0281$05.00

of resolution. This review deals primarily with the new structural information that has emerged since these developments. Not only has this structural framework added a dimension to the study of catalytic mechanisms and inhibitor specificity, but it has also enabled investigators to extend the interpretations of earlier studies where conclusions were arrived at without benefit of a structural template.

The reader should refer to other reviews for complementary or background information. Classic though somewhat dated reviews detail catalytic mechanisms (11), biochemical and catalytic properties (11, 12), and genetics of the cholinesterases (13, 14). Recently, short overviews (15, 16) and an exhaustive review (17) with a perspective on structure have been written. A recent monograph details several of the ongoing research events in the field (18).

THE CHOLINESTERASE FAMILY OF PROTEINS

The initial sequence of cholinesterase showed no global amino acid homology with any other serine hydrolases despite similarity of functional parameters and a common pentapeptide sequence around the active center serine (9). Rather, sequence identity was evident between cholinesterase and the carboxyl-terminal region of thyroglobulin (9, 19). This discovery provided the first indication that the cholinesterases defined a new family of serine hydrolases and that this gene family possessed an unexpected diversity in that non-hydrolase functions could be subserved by a common structural matrix. Soon after *Torpedo* AChE was cloned, the *Drosophila* cholinesterase gene was located from genetic studies and its sequence determined (20). This was followed by a butyrylcholinesterase (BuChE) sequence determined by amino acid sequencing (21) and by molecular cloning (22, 23). Mammalian AChEs proved more intractable, but in 1990 the mouse, bovine, and human enzyme sequences were completed (24–26). Other cholinesterase sequences, rabbit BuChE (27), rat AChE (28), *Anopheles* cholinesterase (29), and chicken AChE (30) have been reported. Distinct hydrolases from *Dictyostelium* (31, 32), *Drosophila* and other insects (33–36), the fungi *Geotrichum* and *Candida* (37), and mammals show sequence identities. Included in the mammalian group are microsomal carboxyl esterases (38, 39), lysophospholipase (40), and cholesterol esterase (41). Other proteins, while apparently not similar in primary structure, show a common folding pattern termed the α/β hydrolase fold (42). Included in this group are a wheat carboxypeptidase with a serine hydrolase mechanism (43), dienelactone hydrolase (44), and haloalkane dehalogenase (45).

In addition, members of the tactin family, glutactin and neurotactin, are homologous to the cholinesterases, but like thyroglobulin lack hydrolase activity (46, 47). No mammalian homologue of the tactins is yet known,

but in *Drosophila* tactins are believed to function in establishing contacts between heterologous cells during development. In short, a functionally eclectic family of proteins has emerged whose functional capacities extend well beyond simple hydrolase function (Figure 1). Several recent reviews have tabulated sequence identities within this family (42, 48, 49).

Since the initial AChE cloning relied on amino acid sequence to obtain oligonucleotide probes, the disulfide bond profile was established not long after in AChE (50) and BuChE (51). Labeling with radioactive DFP distinguished the catalytic serine, S_{200} (52). The histidine, H_{440}, involved in the catalytic triad was established through mutagenesis (53), but the third component in the triad, a diacidic amino acid, E_{327}, was not defined until the crystal structure was solved (10). All members of the family possess histidine in the 440 reference position, while either glutamate (as in the cholinesterases) or aspartate is found at the position corresponding to E_{327}. Corresponding residues to E_{327} and H_{440} can be found in the hydrolases of this series; however, in some cases, the alignments require liberty in gapping the residues. The three disulfide loops (50, 51) are conserved in several proteins in the family (all cholinesterases and the *Dictyostelium* proteins); others contain the amino-terminal two loops while *Culex* Est B and juvenile hormone esterase contain only the most amino-terminal loop. The third loop present in the cholinesterases, in addition to containing the histidine of the catalytic triad, functions in intersubunit contacts forming a four-helix bundle involved in subunit association (10). An additional cysteine is found very near the carboxyl-terminus that is involved in intersubunit disulfide bonds.

Intersubunit disulfide bonding occurs with identical catalytic subunits to form dimers; typically, noncovalent associations of dimers form homomeric tetramers. Heteromeric oligomers also form between the catalytic subunits and either a lipid-linked subunit or a collagen-containing subunit. These species are shown in Figure 2*A*. In mouse AChE one splicing variant does not contain a carboxyl-terminal cysteine, resulting in a monomeric enzyme species. In some cholinesterases, an eighth cysteine is found as a free sulfhydryl in variable locations. Its role in situ is unknown, but it proved invaluable for obtaining crystals of heavy metal derivatives of *Torpedo* AChE (10).

RELATIONSHIP OF PROTEIN STRUCTURE TO GENE ORGANIZATION

A comparison of protein and gene structures of the cholinesterases from different species provides additional insights into structure-function relationships. Typically, the cholinesterases have been defined as AChEs (EC 3.1.1.7) and BuChEs (EC 3.1.1.8). The latter have broad specificity with

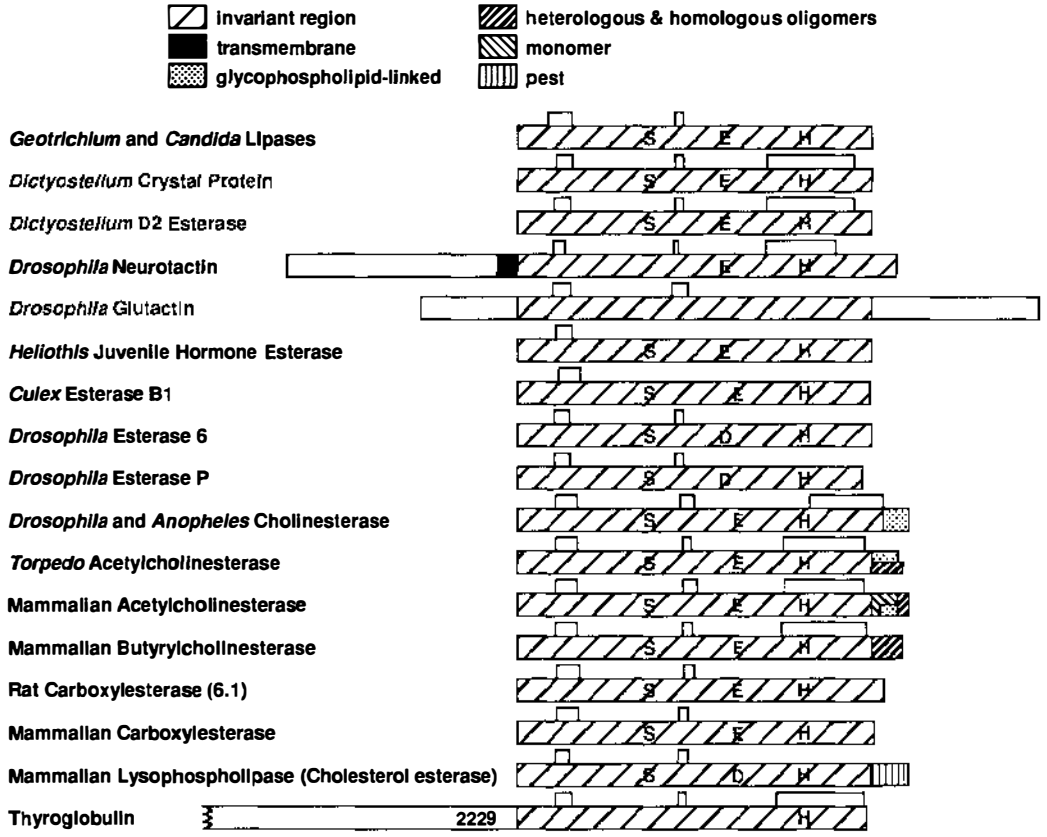

Figure 1 Relationships of some of the proteins with sequence similarities to the cholinesterases. The serines, histidines and glutamates in homologous positions to S_{200}, H_{440}, and E_{327} in *Torpedo* acetylcholinesterase are shown. Intrasubunit-disulfide bonds are shown by the bracketed loops above the sequence (modified from Ref. 16).

respect to the size of the substrate acyl group, while for AChE, a marked reduction in catalysis is seen between propionylcholine and butyrylcholine (54). Over the decades several selective inhibitors for AChE and BuChE have been found (55).

Drosophila appears to harbor only a single cholinesterase gene, which has features of both the AChEs and BuChEs in its encoded protein sequence (20). Similarly, its catalytic specificity is also intermediate between the two enzymes (56). Hence, it seems likely that the acetyl and butyryl subtypes of cholinesterase, which are found in lower vertebrates (57), diverged in the broad time frame between insects and lower vertebrates. Interestingly, genetic and biochemical evidence suggests multiple cholinesterase genes, perhaps three, in *Caenorhabditis elegans* (58, 59). Since the *C. elegans* genes have not been cloned, ancestral relationships in terms of sequences and specificity have yet to be ascertained.

Genomic clones of *Drosophila* cholinesterase (20), *Torpedo* AChE (60), human AChE (61), mouse AChE (61), and human BuChE (62) have been isolated. The *Drosophila* gene contains multiple exons, whereas *Torpedo* and mammalian AChE genes have relatively simple organizations. At present, our knowledge of AChE gene organization is more advanced than for BuChE, and there is as yet no evidence for alternative splicing of the BuChE gene. The open reading frame of human BuChE gene is encoded in over 50 kb of sequence and contains very large introns, whereas the comparable region in the mammalian AChE genes are encoded within 4.5–4.7 kb. The *Torpedo* AChE gene is larger; it requires 25 kb of sequence. However, the exon-intron junctions are identical in the open reading frames for AChE and BuChE, except for an additional intron located between exons 2 and 3 in mammalian AChE (Figure 2*B*).

Alternative mRNA processing is found at the 5′ and 3′ ends of the AChE gene (60, 61, 63–67), but only the splicing at the 3′ end of the open reading frame is responsible for the various molecular species of AChE. This splice occurs at amino acid 535 in the *Torpedo* sequence (68) and at 543 in mouse and human (61). Splicing in *Torpedo* gives rise to two splice alternatives, a hydrophilic peptide of 40 amino acids in length and a hydrophobic peptide of 38 amino acids; the latter appears to be cleaved after cysteine 537 with the concomitant addition of a glycophospholipid. A cDNA clone isolated from *Torpedo marmorata* has raised the possibility of a continuation of exon 4 into the retained intron (64); however, the existence of this mRNA species or the gene product awaits documentation.

In the mouse enzyme two splicing alternatives give rise to a hydrophilic species: either splicing exon 4 to exon 6 yielding a cysteine containing a 40-amino acid peptide or a direct extension into the retained intron yielding a 30-amino acid extension devoid of a cysteine (61). Hence, the latter

A

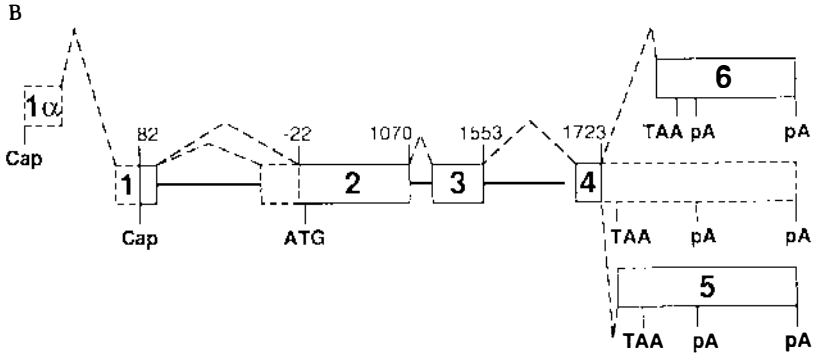

Figure 2 (*A*) Molecular species of acetylcholinesterase. The species are divided into two classes: a heteromeric class consists of catalytic subunits disulfide bonded to either a lipid-linked subunit or a triple helix of collagen-containing subunits. The homomeric class exists as monomers, dimers, and tetramers and can be divided to the hydrophilic or amphiphilic (glycophospholipid-linked) forms. The alternative exons that give rise to the various molecular species are also shown. Nomenclature designating hydrodynamic properties (A = asymmetric and G = globular) and number of catalytic subunits is also shown (17). (*B*) Structure of the genes encoding mammalian acetylcholinesterase and the exon numbering system. Alternative exon splices are shown by the dotted lines. The transcriptional start sites (Cap), translational start site (ATG), translational stop signals (TAA), and polyadenylation signals (pA) are also marked (modified from Ref. 16).

species should only exist as a monomer. The glycophospholipid-linked species in mouse and human are encoded by splicing exon 4 to exon 5 yielding 43- and 42-amino acid peptides, respectively, at their carboxyl-termini. All but 14 of the amino acids are cleaved with the addition of a glycophospholipid (24, 61). mRNA protection and expression studies verify the existence of such species in intact tissue and in transfected cells (66, 67). Hence, AChE contains a constant catalytic core consisting of the first 543 amino acids in mammals or 535 amino acids in *Torpedo,* which are encoded within three exons in mammalian AChE and two exons in *Torpedo* AChE. In mammalian BuChE the open reading frame is encoded in two exons. In this region is found the essential catalytic residues required for activity. The alternatively spliced regions in AChE only encode the remaining few amino acids (from 2 to 40) at the very carboxyl-termini of the respective processed enzymes. This domain governs intersubunit linkages and the cellular dispositions of the enzymes.

Avian AChE shows an interesting variant on this theme since it contains additional coding sequence at the position between exons 2 and 3 in the mammalian enzyme (30). The included sequence gives rise to a 20-kd increase in molecular mass of the enzyme. Variations in this region are responsible for the polymorphism of molecular weight seen in AChE from

quail (69). Alternative splicing giving rise to cholinesterases with distinct carboxyl-termini have yet to be found in the avian AChE or in BuChE from any species.

Although early studies indicated a greater complexity in the cholinesterase genes, mammalian AChE (61), avian AChE (69), and mammalian BuchE (62) are apparently each encoded by single genes. The human AChE gene is localized to 7q22 (70, 71) and human BuChE to 3q26 (71–73). The mouse gene is found at the distal end of chromosome 5, an area of synteny with 7q (74).

THREE-DIMENSIONAL STRUCTURE OF ACETYLCHOLINESTERASE

Crystallographic Analysis

The dimeric, glycophospholipid-linked form of *Torpedo* AChE was treated with phosphatidylinositol-specific phospholipase C to yield a soluble form of the enzyme amenable to crystallization (75). A structure at 2.8Å resolution has been solved and crystals suitable for higher resolution studies are available (10). Three amino acids at the amino- and carboxyl-termini, the noncleaved portion of the glycophospholipid, and a very short exposed loop, residues 485–489, showed sufficient disorder to preclude detection.

The subunits contain a 12-stranded β-sheet surrounded by 14 α-helices. They are ellipsoid in shape (45 × 60 × 65Å) and associate as dimers in a four-helix bundle. A tetramer of *Electrophorus electricus* AChE has also been crystallized (76). A low resolution structure revealed a subunit arrangement of a dimer of dimers.

Identities in Folding Patterns

The structure of *Geotrichum* lipase, an enzyme homologous in sequence, became known at about the same time as that for *Torpedo* AchE (77). These two enzymes show the same folding pattern and also contain the identical positional alignments of the Glu, His, and Ser catalytic triad discussed below. A common folding pattern is seen in the cholinesterase family (10, 49), termed the α/β hydrolase fold (49); it consists of the β_1 through β_8 sheets and the connecting α-helices. Surprisingly, a serine carboxypeptidase from wheat, a dienelactone hydrolase from *Pseudomonas,* and a haloalkane dehalogenase from *Xanthobacter* also show the same folding pattern, despite the absence of sequence identity. Even with the disparities in sequence, the structures of these proteins have converged to position the catalytic triad not only in the same three-dimensional configu-

ration but also at corresponding positions in the turns at the ends of the β-sheets and α-helices.

Modeling of Other Cholinesterase Structures

AChE and BuChE exhibit 51–54% amino acid residue identity and modeling of BuChE on the basis of the AChE structure has been carried out, yielding a virtually identical configuration of the peptide backbone (78). Conservation of the intrasubunit disulfide bond positions and the conservation of the α/β hydrolase fold, despite considerable variations in primary structure, suggest that modeling will provide a useful framework for structural studies of other proteins in the homologous series.

The Active Center and Catalytic Triad

The crystal structure established that a E_{327} H_{440} S_{200} triad with appropriate hydrogen bonding distances and alignment was at the base of a narrow gorge 20Å in depth (10). Such triads, involving a dicarboxylic amino acid withdrawing a proton from a serine through the imidazole of histidine, are characteristic of the other families of serine hydrolases. This arrangement in the cholinesterases and *Geotrichum* lipase differs from other serine hydrolases in two respects: most enzymes in the cholinesterase family use a glutamate instead of the aspartate found in the previously characterized serine hydrolases to supply the negative charge; and the steric arrangement of residues in AChE is the mirror image of the pancreatic serine hydrolases (10). Otherwise, orientation of the side chains and hydrogen bond distances show the side chains of the triads virtually superimposable in three-dimensional space.

The gorge is lined with 14 aromatic residues. Some are deep within the gorge while most others define a large aromatic patch on the wall of the gorge. Just below the rim of the gorge lies D_{72}, at the base of the gorge lies E_{199}, and deeper into the molecule lies D_{443}. Several other anionic residues are located farther from the gorge. E_{199} is the closest anionic side chain to contact distance with trimethylammonio group acetylcholine when bound. A single negative charge at the base of the gorge seems inconsistent with a rate acceleration for binding of cationic ligands ascribable to the presence of 6–9 negative charges (79, 80). However, a global analysis of surface potentials (81) and of the orientation of the molecular dipole intrinsic to AChE with respect to the active center gorge (82) predict substantial charge accelerations for cationic substrates or inhibitors entering the gorge. Various hypotheses have also been proposed regarding the role of aromatic residues in the gorge [aromatic guidance, (10)] that facilitate diffusion of the substrate to the active center. The aromaticity may also preclude the necessity of displacement of slow-exchanging water molecules at the base

of the cleft upon ligand binding and hence it could simply play a passive role. BuChE contains six fewer aromatic residues within its gorge, yet exhibits only a threefold reduction in catalytic efficiency, as measured by k_{cat}/K_m.

Crystallographic analysis of the AChE-decamethonium and AChE-edrophonium complexes (83, 84) and the positioning of the active center serine near the carbonyl carbon of acetylcholine enable one to model the bound substrate and perform experiments on energy minimization docking. Aromatic residues clearly play an important role in stabilization of the complex. The choline moiety appears to be stabilized by W_{84} and F_{330} in AChE whose orbitals lie close to the trimethylammonio surface, as defined by its van der Waal's radii. Also, the van der Waal's surfaces of choline and E_{199} are found within 1–2Å of each other.

Several considerations allow estimation of the free energy contributions stabilizing a bound quaternary group. Studies of neutral substrate interactions with AChE (85, 86), the synthesis of cage-like compounds containing aromatic residues to stabilize quaternary ammonium ligands (87), and the crystal structure of phosphorylcholine-antibody complexes (88) all point to a role for aromatic residues being in close apposition to the quaternary moiety in the stabilization of this diverse set of complexes. However, this argument can be carried too far if longer-range electrostatic forces are ignored. In fact, both electrostatic (Coulombic) and hydrophobic forces are likely to contribute to stabilization of the complex. The approach of partitioning free energy to both the electrostatic and hydrophobic force contributions to a quaternary ligand binding site was made almost a half-century ago by Pauling and colleagues when they compared energetics of binding of phenyltrialkylammonium ions to an antibody raised to quaternary ligands (89).

As we continue around the binding site for acetylcholine (Ach), the active site serine hydroxyl should be positioned close to the carbonyl carbon on Ach. In turn, the carbonyl oxygen should be stabilized through hydrogen bonding to two amide backbone hydrogens at positions 119, 121, and/or 201 (10). A clear delineation of the acyl pocket is provided by the side chains of F_{288} and F_{290} pointing inward toward the binding site. These two residues would be expected to constrain the dimensions of the acyl pocket in AChE (Figure 3).

The Peripheral Anionic Site

J.-P. Changeux proposed an allosteric mechanism of inhibition of AChE nearly 30 years ago. He examined the inhibition of steady state kinetic parameters by various inhibitors and inhibitor combinations (90). A periph-

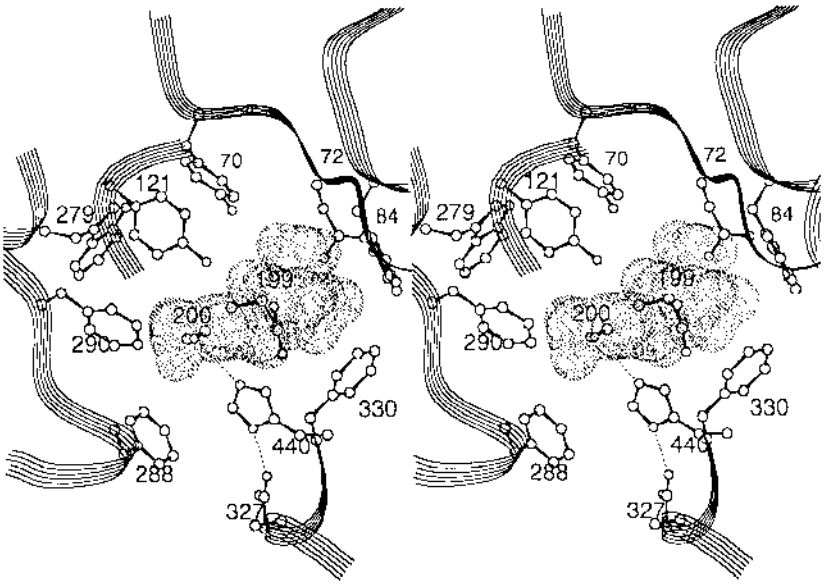

Figure 3 Structure of *Torpedo* acetylcholinesterase showing the positions of critical side chains and bound acetylcholine positioned by energy minimization (131, 132). (*a*) The catalytic triad: S_{200}, H_{440}, E_{327}. (*b*) The choline binding subsite: W_{84}, Y_{330}, E_{199}. (*c*) The acyl pocket: F_{288}, F_{290}. (*d*) The peripheral anionic site: Y_{70}, Y_{121}, W_{279}, D_{72}.

eral site, which likely gives rise to allosteric inhibition, was subsequently identified by direct titrations with the fluorescent inhibitor, propidium (91: see inset for structures). Criteria such as (*a*) the inability of agents that phosphorylate the active center serine to alter propidium binding; (*b*) the capacity of reversible inhibitors such as edrophonium and N-methylacridinium, which bind at the active center, to associate with AChE simultaneously with propidium to form ternary complexes; and (*c*) the mode of propidium inhibition of AChE acylation by substrates all point to a peripheral anionic site for thc binding and allosteric actions of this inhibitor (91, 92). Moreover, measurements of fluorescence energy transfer between certain fluorescent alkyl phosphonates and propidium suggest that approximately 20Å separate the excited state dipoles between the alkylphosphate donor and the propidium acceptor of resonance energy transfer (92). Labeling studies using propidium to protect labeling by a photoactive reagent, DDF (93), and direct labeling by azidopropidium (94), have identified two sets of peptides (residues 270–278 and 251–266 in *Torpedo*) that should contribute to the binding surface of the peripheral anionic site. Finally, a terpyridine platinum coor-

dination complex acts in a manner similar to propidium as an inhibitor and labels H_{280} in human AChE (95). The locations of the exposed surface of these residues are near the rim of the active center gorge. Hence, ligand association with the peripheral site may prevent access of substrates to the gorge by physical obstruction to restrict entry to the gorge, by charge repulsion imparted by the association of a cationic ligand, or by an allosteric mechanism in which the active center conformation is altered. In this connection, it is noteworthy that the cationic Pt-terpyridine complex inhibits catalysis of acetylcholine to a greater extent than neutral substrates (95).

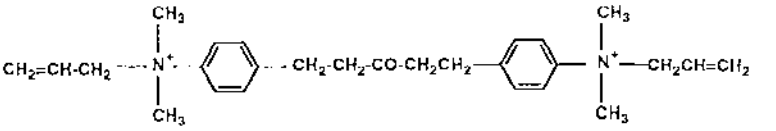

BW284C51

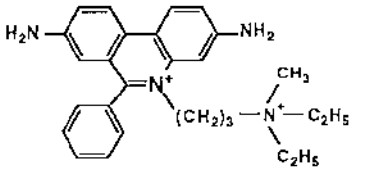

Propidium

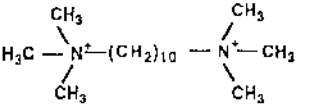

Decamethonium

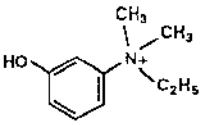

Edrophonium

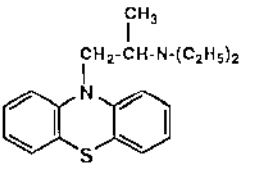

Ethopropazine

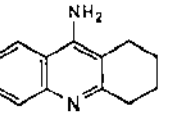

Tetrahydro-9-aminoacridine
(Tacrine)

Three related peptide snake toxins of the fasciculin family bind to mammalian and *Torpedo* AChE but not to avian AChE or mammalian BuChE with K_Ds in the picomolar range (96, 97). These peptides of 6500 Da bind to AChE phosphorylated with DFP, but binding is prevented by propidium and certain *bis*-quaternary inhibitors. Hence, fasciculin emerges as a strong candidate for binding to the peripheral site on AChE as well (96, 97).

The function of the peripheral anionic site in catalysis in vivo and its role in synaptic activity remain open issues. It may be involved in forming

an initial complex to facilitate substrate transfer down the gorge (95). Competition between high concentrations of substrate and propidium suggest a role in substrate inhibition (98), and it has been proposed that the site serves as a sensor to maintain constant catalytic rates over a range of ionic strengths (99). Several *bis*- and *tris*-quaternary ligands bind to the peripheral site, and *bis*-quaternary ligands with large interquaternary distances (~14Å or greater) prevent the binding of both active center and peripheral site ligands (91, 92). Steric overlap between the *bis*-quaternary ligand with ligands selective for the peripheral and active sites could be responsible for this mutually exclusive binding.

Molecular Basis of Ligand Specificity at the Active Center

The dimensions of the active center gorge determined from X-ray crystallography (10) and chemical modification studies help to elucidate the specificity and orientation of bound ligands.

Early studies of Wilson & Quan (100) demonstrated the importance of a *meta* hydroxyl group in enhancing the inhibition capacity of phenyl trialkylammonium ligands. The crystal structure of the edophonium-AChE complex shows that the hydroxyl group bisects the hydrogen bond between the imidazole nitrogen in H_{440} and the serine hydroxyl group (S_{200}) and should alter the hydrogen bonding scheme (83). In addition, the aromatic ring of edrophonium is stabilized through π orbital overlap with W_{84} and, perhaps, F_{330}. The role of this site in binding of quaternary ammonium groups was also established by chemical labeling experiments where edrophonium selectively protects DDF labeling of peptides containing W_{84} in *Torpedo* (101) and presumed a peptide in *Electrophorus* AChE homologous to F_{330} (84, 102). Longer-range electrostatic interactions also appear to play a role. E_{199} resides at the base of the gorge and the distance separating the van der Waals radii of its carboxylate oxygen and the quaternary methyl groups is within 1.5Å.

Tricyclic ring-containing inhibitors such as tacrine (tetrahydro-9-aminoacridine, see inset for structures) occupy a location similar to that of edrophonium, although further rotation of the F_{330} side chain to accommodate an aromatic ring in the complex between tacrine and AChE is evident (83, 84). The tricyclic ring system inserts between F_{330} and W_{84}, causing increased stabilization by virtue of the π-orbitals. Early studies provided evidence for a charge-transfer complex between N-methylacridinium and a tryptophan in AChE (103). Moreover, the binding of N-methylacridinium and 3-aminopyridinium-1,10 decane results in near complete quenching of their fluorescence upon binding (104). The role of the indole side chain in W_{84} in acridinium binding seems clear in that it should provide the electron-rich donor ring system for association with the cation-containing

ring acceptor of acridinium. This tryptophan may well account for the changes mentioned above in absorption and fluorescence spectra typical of a charge-transfer complex.

The tricyclic ring system must not completely occlude the nucleophilic serine or the alignment of the other members of the catalytic triad since Barnett & Rosenberry found that thc binding of these compounds can actually augment catalysis of neutral substrates such as ethylacetate (105). Accordingly, charge neutralization and the insertion of an aromatic ring system within the cleft enhance the catalytic surface for neutral ester substrates provided the size of the alcohol portion of the ester is kept small. Given the steric constraints of the gorge, the finding becomes even more intriguing and may argue for intrinsic flexibility within the gorge.

The portion of the active center accommodating the acyl portion of the substrate reveals that two phenylalanines, F_{288} and F_{290}, have their side chains directed into the active center and, as such, define the steric constraints of thc active center. In BuChE, the conserved phenylalanines are replaced with L and I or V, providing a hydrophobic but less dimensionally constrained acyl pocket. Presumably, the phenylalanine side chains account for the marked fall-off in AChE catalysis in going from propionylcholine to butyrylcholine (54), the specificity of certain organophosphates (i.e. isoOMPA) for butyrylcholinesterase (55) and the marked stereospecificity seen with organophosphate inhibition of AChE when the moieties attached to the phosphorus differ greatly in molecular dimensions (106). Such observations would also predict that the stereoselectivity of organophosphate reactions with BuChE are much lower than with AChE.

Site of Bis-*Quaternary Ligand Association*

The site of *bis*-quaternary ligands possessing large interquaternary distances can be ascertained, in part, from kinetic studies. Early studies by Belleau and colleagues (107, 108) and by Wilson and colleagues (109) demonstrated that *bis*-quaternary and some monoquaternary inhibitors actually enhance the rate of acylation of the enzyme by neutral substrates. This enhancement is indicative of the *bis*-quaternary ligand-enzyme complex maintaining access to the active center serine for acylating agents and perhaps altering conformation of the active center to affect reactivity. In addition, series of *bis*-quaternary ligands were examined for their capacities to bind to the sulfonylated and phosphorylated AChEs (110). Only when the phosphorylating agent or the groups surrounding the ammonio group in the quaternary ion became bulky did modification of the active center serine by phosphorylation or sulfonylation affect the affinity of the *bis*-quaternary ligand (110). In addition, *bis*-quaternary ligands bind in a mutually exclusive manner with ligands selective for the active center (i.e. edrophonium and N-methylacridinium) and the peripheral site

(propidium, gallamine, and d-tubocurarine). The simplest explanation would suggest an overlap of binding surfaces. Since the interquaternary extension between the nitrogens in decamethonium is ~14Å and the two trimethylammonio groups will add another 6Å in length, the potential spanning distance is large. The crystal structure of the AChE-decamethonium complex shows one trimethylammonio group lodged between F_{330} and W_{84}; the other extends out of the active center gorge and is enlodged in the vicinity of W_{279}, Y_{70}, and Y_{121}, which reside near the lip of the gorge (83, 84). The latter residues have also been implicated in binding at the peripheral anionic site (10, 92–94). Studies with spin-labeled *bis*-quaternary ligands show immobilization of both ends of the bound molecule and a separation between the ammonio-linked nitroxides consistent with an extended bound conformation (111). Other *bis*-quaternary fluorophores have further defined the characteristics of the ligand binding site (111a).

A self-consistent picture of the binding loci of the active center, peripheral anionic site, and *bis*-quaternary ligands is emerging. Having identified the major domains in the molecule responsible for specificity, their precise roles in catalysis and in the energetics of inhibitor binding have been analyzed further through mutagenesis and molecular modeling. These studies are detailed in a subsequent section.

CATALYTIC PARAMETERS AND MECHANISMS

The catalytic potential of the cholinesterases is wide ranging with oxyesters, thioesters, selenoesters, amides, anilides, carbamoylesters, and phosphorylesters all being susceptible to catalysis (11, 12, 17, 112). Often the range of substrate catalytic potential goes unrecognized owing to the high rate of acetylcholine turnover ($k_{cat}/K_m = 10^8 M^{-1} sec^{-1}$) and the 10^{14} enhancement of enzyme catalyzed over H_2O catalyzed ester hydrolysis for the efficient substrates (113, 114).

A general scheme for catalysis can be represented for an ester or related substrate designated by AcOR:

$$\text{E-OH} + \text{AcOR} \underset{k_{-1}}{\overset{k_1}{\rightleftharpoons}} (\text{E-OH}\cdots\text{AcOR}) \xrightarrow{k_2} \text{E-OAc} + \text{ROH} \xrightarrow[H_2O]{k_3} \text{E-OH} + \text{AcO}^- + \text{H}^+$$

acylation *deacylation*

Scheme 1

In the above scheme formation of a reversible complex with an acyl ester

is followed by acylation to form E-OAc represented by the first order rate constant k_2, and then deacylation, represented by the first order rate constant, k_3. The general features of the catalytic cycle of acylation and deacylation have been widely studied in the serine hydrolases. Serine 200 is likely to be rendered more nucleophilic by the catalytic triad. Formation of the acyl enzyme proceeds through formation of a tetrahedral intermediate which relaxes back to the trigonal, acyl enzyme. The imidazole in H_{440} may also assist by accepting the released proton. Deacylation also proceeds through a tetrahedral intermediate by attack of the acyl-enzyme bond from an internal H_2O. The H_2O may be rendered more nucleophilic by a neighboring carboxylate or imidazole residue.

In the above scheme,

$$k_{cat} = \frac{k_2\, k_3}{k_2 + k_3} \qquad \text{(Equation 1)}$$

$$K_m = \frac{k_{-1} + k_2}{k_1} \cdot \frac{k_3}{k_2 + k_3} \qquad \text{(Equation 2)}$$

$$\frac{k_{cat}}{K_m} = \frac{k_1 \cdot k_2}{k_{-1} + k_2} \qquad \text{(Equation 3)}$$

k_{cat} is governed by the energy barriers for acylation and deacylation and is the geometric mean of the two rate constants. K_m equals the equilibrium constant for the initial association only when $k_3 \gg k_2$ and $k_{-1} \gg k_2$. k_{cat}/K_m measures the initial steps leading up to formation of the acyl enzyme. Attempts to trap the acyl intermediate suggest that acylation and deacylation occur at comparable rates at V_{max} (115). This, in turn, indicates that k_2 and k_3 are of comparable magnitude for acetylcholine. For acetylcholine, k_{cat} approaches 10^4 sec^{-1} and $K_m = 5 \times 10^{-5}$ M. Accordingly, $k_{cat}/K_m = 2 \times 10^8$ M^{-1} sec^{-1}, a value approaching the diffusion limitation for k_1 (80, 114, 116).

AChE catalyzed hydrolysis of ACh and its thiol ester analogue acetylthiocholine (ATCh) approaches catalytic perfection (117) and under such conditions we might expect the transition state barriers for diffusion, acylation, and deacylation to be roughly equivalent. Hence, over a large concentration range, diffusion of substrate to the active center denoted by k_1 is essentially rate limiting.

By contrast, neutral esters and other less optimal substrates may require an induced fit to achieve acylation. Under such conditions, k_1 might be divided into two (or more) steps where k_a now reflects the diffusion step and k_b induced fit to optimize substrate orientation (118).

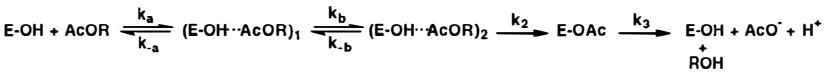

Scheme 2

In this situation:

$$\frac{k_{cat}}{K_m} = \frac{k_a\, k_b\, k_2}{k_2\,(k_{-a} + k_b) + k_{-a}\, k_{-b}} \qquad \text{(Equation 4)}$$

For a common acyl group, deacylation rates should be the same; hence, we may find sets of substrates where the *a* step of diffusion of reactants or the *b* step of isomerization is rate limiting. Rosenberry (118) and Quinn and colleagues (114, 116, 119) have examined the influence of pH and fraction of deuterated substrate (isotope inventories) on catalytic parameters to deconstruct Michaelis-Menten parameters into individual rate constants and ascertain rate-limiting steps. For example, linear proton inventory plots for v/K_m have been observed for various acyl esters, which indicate that a single proton transfer rather than transfer of multiple protons is involved in the rate-limiting step of the reaction (119). Hence, no evidence can be adduced for a charge-relay system or multifunctional proton transfer in the reaction (119). The pH dependences also indicate that the rate-limiting step changes between efficient and poor substrates (118) and between ACh and benzoylcholine (116). Efficient substrates such as ACh are limited by diffusion of substrate, while others may depend either on isomerization steps leading to acylation or the acylation step itself.

In the extreme case for carbamoylating and phosphorylating agents, deacylation or the k_3 step is rate limiting in turnover. Effectively, these agents become hemisubstrates when the observation times become shorter than the deacylation half-lives.

Substrate Inhibition and Activation

Since the comprehensive studies of Augustinsson in the 1940s (54), substrate inhibition has been a hallmark of cholinesterase catalysis. It has been sufficiently characteristic to use it as a means of distinguishing AChEs from BuChEs. The mechanism of substrate inhibition is not well resolved and, in fact, data do not clearly distinguish between influence occurring on the acylation or deacylation step (98, 112, 120). If we consider the overall scheme:

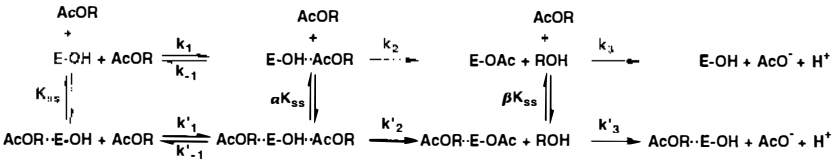

Scheme 3

If excess substrate affects acylation $k_2 \neq k_2'$, while an influence on the deacylation sequence is reflected in $k_3 \neq k_3'$. For substrate inhibition either $k_2' < k_2$ or $k_3' < k_3$. Values of k_2' or $k_3' = 0$ denote excess substrate causing complete inhibition. The BuChEs (121–123) and certain mutations of AChE (123) show substrate activation. If activation and inhibition are occurring through substrate binding to a common site, we might expect both to be dependent on similar sets of residues in the molecule.

SITE-SPECIFIC MUTAGENESIS—CHOLINESTERASE CHIMERAE

Mutagenesis studies in the absence of a three-dimensional structure were largely restricted to residues where sequence conservation, sequence proximity, or a natural mutation suggested a role in function (53, 124–126). The report of a crystal structure added a new dimension as well as a flurry of activity in this arena of investigation.

Expression Systems

Initial studies of mutagenesis were done by mRNA injections into oocytes (125, 127) and transient transfections of cDNA into a receptive cell such as COS (53) or HEK cells (128). mRNA injection of single cells is labor intensive and the limited expression has not permitted a detailed analysis of kinetic and inhibition parameters. Similar limitations apply to transient transfections, particularly in the case of the *Torpedo* enzyme, where efficient protein folding does not occur at 37°C (53, 126) and expression at lower temperatures compromises cell viability. Although the high turnover rates of the cholinesterases facilitate their detection, details of substrate inhibition are only revealed at high substrate concentrations (10–100 mM). At substrate concentrations well above the K_m (~50 μM) general base catalysis of the esters will contribute substantially to basal ester hydrolysis.

Determinations of k_{cat} or k_{cat}/K_m, as measures of turnover and catalytic efficiency, necessitate titrations of stoichiometry of active sites. This entails antibody precipitation to determine total cholinesterase protein, ascertaining

active center concentrations with high-affinity phosphorylating agents or purifying the enzyme to homogeneity. Each approach has particular advantages and limitations.

Stable transfectants of mammalian embryonic cell lines have yielded expression levels about an order of magnitude higher than transient transfection (129, 131). Finally, expression systems in baculovirus-*Spodoptera* (132) and *Escherichia coli* (133) have produced 3 mgs and over 100 mg of enzyme per liter of culture system, respectively. However, the former system presents difficult cloning steps to achieve expression, while in the latter system, generation of active enzyme required denaturation followed by refolding. Only ~3% of the enzyme renatured as an active entity.

Kinetic Parameters for Mutant Enzymes

The ratio k_{cat}/K_m, a second-order rate constant, is typically used as the measure of catalytic efficiency to compare mutant enzymes. This ratio reflects the catalytic through put under nonsaturating conditions while k_{cat} reflects maximal turnover. To describe substrate inhibition, two constants, K_m and K_{ss}, represent the concentration-dependence of catalysis and inhibition by excess substrate. An additional parameter, b, has been incorporated into kinetic schemes (112) to reflect the maximal extent of inhibition or activation by excess substrate with the mutant enzymes (123).

In a scheme where we do not differentiate whether binding of a second substrate molecule affects acylation or deacylation and $K_{ss} = \alpha K_{ss}$,

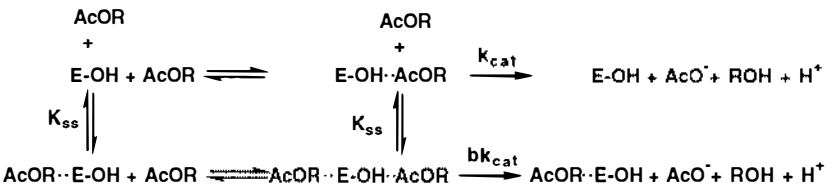

Scheme 4

then

$$v = \frac{1 + b\,[S] / K_{ss}}{1 + [S] / K_{ss}} \cdot \frac{V_{max}}{1 + K_m / [S]} \qquad \text{(Equation 5)}$$

when $b = 0$,

$$v = \frac{V_{max}}{1 + [S] / K_{ss} + K_m / [S] + K_m / K_{ss}} \qquad \text{(Equation 6)}$$

Hence, in this scheme substrate inhibition is described in terms of the dissociation constant for the inhibitory site, K_{ss}, and the relative efficiency of the ternary versus the Michaelis-Menten complex to acylate and deacylate substrate, b. This scheme is also applicable to substrate activation where $b > 1$ rather than $b < 1$. When $b = 1$, Michaelis-Menten kinetics are observed.

Reversible inhibition has been evaluated by IC_{50}'s and by measurement of dissociation constants. IC_{50}'s leave considerable uncertainties regarding inhibition mechanisms and the form of the enzyme to which the inhibitor binds. IC_{50}'s for competitive inhibitors are dependent on the K_m of the substrate relative to the substrate concentration, whereas for noncompetitive inhibitors they are independent of this ratio. Since K_m's may also be affected by mutations in the enzyme, a change in IC_{50} in the extreme case could reflect a change in K_m and not in K_I for the inhibitor. By contrast, K_I is independent of K_m. A second advantage of ascertaining the inhibition mechanism is that the influence of mutation can be compared for the same species of enzyme in the kinetic scheme. For convenience, the free species without bound substrate (i.e. E-OH) is often used; dissociation of its complex is reflected in the competitive inhibition constant.

In the case of inhibitors that carbamoylate or phosphorylate the active site serine, IC_{50}'s become parameters of limited applicability to mechanistic considerations or correlating data obtained under different conditions. Data for these inhibitors should be described in terms of a time-dependent parameter and a constant describing the concentration dependence of inhibition.

Summary of Mutation Analyses[2]

Table 1 summarizes the reported cholinesterase mutants by dividing them into several structural domains: (*a*) catalytic triad; (*b*) active center-acyl pocket; (*c*) active center-choline binding subsite; (*d*) peripheral-site(s)—rim of the gorge; (*e*) carboxyl-terminus; (*f*) glycosylation; (*g*) cholinesterase chimeras. The essential observations are detailed below:

CATALYTIC TRIAD Mutagenesis has confirmed the role for the E_{327} H_{440} S_{200} linkage in catalysis (53, 129, 134, 135). Although mutation of several other conserved diacidic amino acids results in inactive enzyme (129, 136), these residues are likely to be critical for folding into a correct tertiary conformation rather than directly involved in the acylation and deacylation steps (136). In fact, recent evidence suggests that a conformation of chicken

[2]Residue identification refers to the species under study. The parentheses refer to the *Torpedo* sequence, which serves as an alignment reference for other enzymes.

Table 1 Cholinesterase Mutations[a]

Enzyme and Residues[b]	*Torpedo* Equivalent	Catalytic, Inhibitor Specificity and Structural Change	Reference
Catalytic Triad			
TA S_{200}A,C	200	A is inactive; C may be inactive or possess 0.1% of wild-type activity	53
HA S_{203}A,C	200		129
HB S_{204}C,T,D,Q,H	200		135
TA H_{440}Q	440	Inactive; AChE with the other conserved histidine mutated is active, H_{425}	53
HA H_{447}A	440		129
TA E_{327}Q,D	327	Inactive	134
HA E_{334}D,Q,A	327	Inactive	129
Active Center-Acyl Pocket			
MA F_{295}L	288	↓ ATCh k_{cat}/K_m, ↑ BTCh k_{cat}/K_m; ↑ isoOMPA inhibition rate	131
HA F_{295}L,A	288	Similar to above	138
HB L_{286}K,Q,R,D	288	↑ K_m, change in inhibitor specificity	135
MA R_{296}S	289	Little change in activity	131
MA F_{297}I	290	↓ ATCh k_{cat}/K_m; ↓ BTCh k_{cat}/K_m; ↑ isoOMPA inhibition rate; K_{ss} ↑, b ↑	131
MA F_{295}Y	288	Little change in substrate specificity	123
MA F_{297}Y	290	↑ K_{ss}	123
DC F_{368}Y,S	290	Increased organophosphate resistance	139
HA F_{297}V,A	290	↓ ATCh k_{cat}/K_m; ↑ BTCh k_{cat}/K_m, ↑ isoOMPA inhibition	138
MA V_{300}G	293	Little change in activity	131
MA F_{295}L, F_{297}I	288, 290	↓ ATCh k_{cat}/K_m; ↑ BTCh k_{cat}/K_m; ↑ isoOMPA inhibition rate	131
HA F_{295}L, F_{297}V	288, 290	↓ ATCh k_{cat}/K_m; ↑ BTCh k_{cat}/K_m; ↑ isoOMPA inhibition	138
TA F_{288}L, F_{290}I	288, 290	↓ ATCh→ ↑ BTCh catalysis; ↑ isoOMPA inhibition	78
MA F_{295}L, F_{296}S, F_{297}I	288, 289, 290	↓ ATCh k_{cat}/K_m	131

Table 1 (*Continued*)

Enzyme and Residues[b]	*Torpedo* Equivalent	Catalytic, Inhibitor Specificity and Structural Change	Reference
Active Center—Choline Binding Site			
HA $Y_{337}A$	330	↓ substrate inhibition	130
MA $Y_{337}A,F$	330	Change in inhibitor specificity (esp. A)	123
TA $E_{199}Q,D$	199	↓ k_{cat}/K_m ↓ substrate inhibition (esp. D), change in inhibitor specificity, diminished aging rate	132, 53, 166
HA $E_{202}Q,D,A$	199	↓ k_{cat}/K_m ↓ substrate inhibition, change in inhibitor specificity	130
HA $W_{86}A$	84	↓ k_{cat}/K_m ATCh, ↓ propidium affinity, ↓ edrophonium affinity	130, 138
HB $Y_{440}D$	442	↑ K_m; change in inhibitor specificity	135
Gorge Entry (Peripheral Anionic Site)			
HA D_{74} E,N,G,K	72	↓ *Bis*quaternary, propidium, and dibucaine inhibition; ↓ Substrate inhibition	129, 130
MA $D_{74}N$	72	↑ K_m ↑ K_{ss}	123
HB $D_{70}G$[c]	72	Succinylcholine and dibucaine inhibition	125, 140
DC $Y_{109}D,G,K$	72	G ↑ preference BTCh K lower substrate affinity	142
TA $W_{279}A$	279	↓ Propidium and *bis*quaternary inhibition	78
HA $W_{286}A$	279	↓ Propidium and *bis*quaternary inhibition	130
MA $W_{286}R$	279	↓ Propidium and *bis*quaternary inhibition	123
MA $W_{286}A$	279	↓ Propidium and *bis*quaternary inhibition	123
MA $Y_{72}N$	70	↓ Propidium and *bis*quaternary inhibition	123
MA $Y_{124}Q$	121	↓ Propidium and *bis*quaternary inhibition	123
MA $Y_{72}N$; $Y_{124}Q$	70, 121	↓ Propidium and *bis*quaternary inhibition	123
MA $Y_{72}N$; $W_{286}R$	70, 272	↓ Propidium and *bis*quaternary inhibition	123
MA $Y_{124}Q$; $W_{286}R$	121, 279	↓ Propidium and *bis*quaternary inhibition	123
MA $Y_{72}N$; $Y_{124}Q$; W_{286}, R,A	70, 121, 279	↓ Propidium and *bis*quaternary inhibition	123
MA $Y_{72}N$; $Y_{124}Q$; $W_{286}R,A$; $D_{74}N$	see above	↓ Propidium and *bis*quaternary inhibition	123

Other Catalytic and Structural Functions			
HB $E_{441}G,E_{443}G$	443, 445	Decreased BTCh catalysis and dibucaine inhibition	140
HA $Y_{114}A$	116	Restores function to D_{70} mutants	140
HB $F_{561}Y$	563	Restores function to D_{70} mutants	140
HB $S_{425}P^c$	427	Associated with D_{70} resistance	125, 140
HB $G_{390}V^c$	392	↓ Succinylcholine, dibucaine and tacrine inhibition	163
HA $H_{322}N^c$	315	YT blood group antigen	161
HA $P_{561}R^c$	541	Allelic variation in glycophospholipid signal sequence	161
HA $F_{338}A$	331	Associates with F_{295}	138, 130
MA $F_{338}G$	331	Associates with F_{295}; ↑ K_{ss}	123
HA Y_{341}	334	↓ Substrate inhibition	138
DC $F_{115}S^c$	78	Increased organophosphate resistance	164
DC $I_{199}V^c$	129	Increased organophosphate resistance	164
DC $G_{303}A^c$	227	Increased organophosphate resistance	164
Intersubunit Association			
TA C_{537}, truncation	537	Secreted	126, 165
HA $C_{580}A$	572	Secreted monomer	128
DC C_{615}, truncation	537	Secreted	145, 146, 151
Glycosylation			
HA $N_{265}Q$	258	Diminished secretion	150
HA $N_{350}Q$	343	Diminished secretion	150
HA $N_{464}Q$	457	Diminished secretion	150
HA $N_{265}Q,N_{350}Q$	258, 393	Greater diminution of secretion	150
HA $N_{256}Q,N_{464}Q$	258, 457	Greater diminution of secretion	150
HA $N_{350}Q,N_{464}Q$	343, 457	Greater diminution of secretion	150
HA $N_{765}Q,N_{350}Q,N_{464}Q$	258, 343, 457	Greater diminution of secretion	150

Table 1 (*Continued*)

Enzyme and Residues[b]	*Torpedo* Equivalent	Catalytic, Inhibitor Specificity and Structural Change	Reference
Chimerae			
TA Exon 4 deletion, exon 3–5 linkage		Glycophospholipid-linked inactive enzyme	126
HB Linkage of mutant and non-mutant enzymes	various	Augments or diminishes influence of the mutant	125, 140
MA Substituted N-terminal and/or C-terminal sequences with BuChE sequence	$B_{1-174}A_{175-575}$ $B_{1-174}A_{175-487}$- $B_{488-575}$	B_{1-174} confers BW specificity of BuChE	131
HB Substituted AChE sequence for BuChE	$B_{1-57}A_{58-133}$- $B_{134-575}$	Imparts partial AChE character	141

[a] MA = Mouse acetylcholinesterase; HA = human acetylcholinesterase; TA = *Torpedo* acetylcholinesterase; HB = human butyrylcholinesterase, DC = *Drosophila* cholinesterase

[b] Other residues, $D_{397}N$ in *Torpedo*, $D_{175}N$, $D_{404}N$ in human have been reported to produce inactive enzyme. $E_{92}Q,L$ results in inactive enzyme in *Torpedo*. Little or no change in activity was reported for $E_{84}Q$, $D_{95}N$, $D_{131}N$, $D_{333}N$, $D_{349}N$ in human and $D_{93}N$ in *Torpedo* (18)

[c] Natural mutations

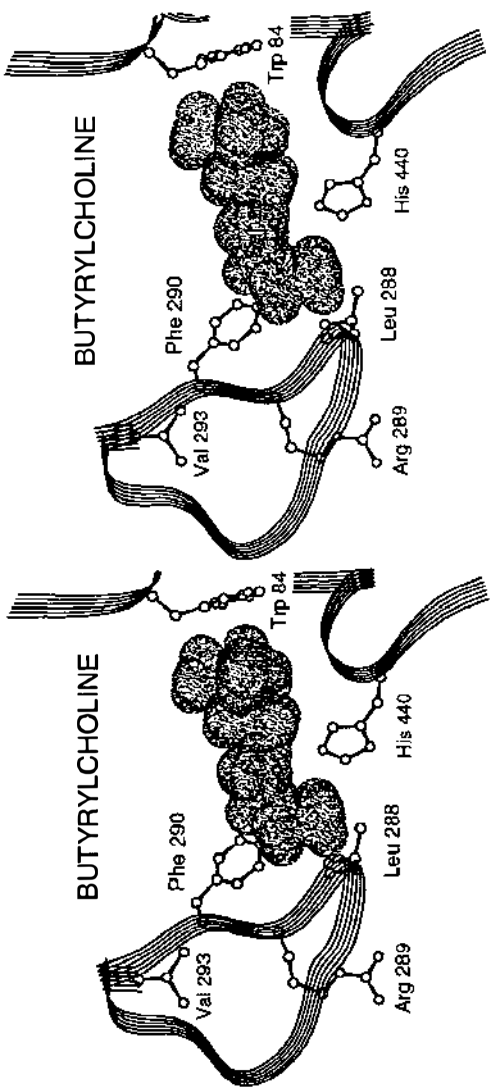

Figure 4 Structure of bound butyrylcholine within the substrate binding site of the F_{288} Mutant ● of Acetylcholinesterase. Energy minimization was done with the Biosym Insight II program (131).

AChE is produced that is DFP reactive, but catalytically inactive towards Ach (137). Whether the catalytically inactive mutants achieve a tertiary conformation approaching the active enzyme or are simply degraded as a nascent peptide chain is unknown. Some mutations of the active center (i.e. $S_{(200)}C$) show low activity (53, 135), and it will be of interest to achieve high expression to analyze them for catalytic properties.

The functional existence of a catalytic triad does not prove the existence of a charge-relay system or rate-limiting proton transfer (119). Rather the optimal alignments of these residues may be critical for confering a proton-withdrawing, inductive effect on the serine and/or a sink capacity for released protons.

ACTIVE CENTER ACYL POCKET Based on the residue differences between AChE and BuChE, the residues outlining the acyl pocket have been substituted in mammalian AChE to produce multiple mutant enzymes (Figure 4). Substitution of $F_{295(288)}$ and $F_{297(290)}$ in AChE to the corresponding residues found in BuChE has increased BuChE character as measured by an increased ratio of butyrylthiocholine (BTCh) to acetylthiocholine (ATCh) catalyzed hydrolysis, changes in the substrate activation and inhibition profiles, and increased susceptibility to inhibition by the BuChE-specific inhibitor, isoOMPA (131, 138). The $F_{295(288)}L$, $F_{297(290)}I$ double mutant (78, 131, 138) and the $F_{295(288)}L$, $R_{296(289)}S$, $F_{297(290)}I$ triple mutant (131) showed similar BuChE character, but were far less active. A detailed analysis of the individual F_{295} and F_{297} mutants uncovered several interesting properties of the acyl pocket. First, the $F_{295}L$ mutant of mouse AChE, while slightly less efficient towards ATCh hydrolysis, hydrolyzed BTCh with a k_{cat}/K_m greater than that found for native BuChE (131). Similar behavior was seen for the human $F_{295}L$ and $F_{295}A$ mutations (138). The $F_{297}I$ mutation is notable in its increased K_m for both ATCh and BTCh and for the elimination of substrate inhibition. In fact, the concentration dependence of BuChE catalyzed hydrolysis of BTCh and ATCh is best described in terms of substrate activation (123, 131) and the F_{297} mutation alone is sufficient to reverse the substrate inhibition in AChE and achieve a large measure of the activation seen with BuChE (123). $F_{338(331)}$, which comes in close proximity to F_{295} through ring stacking, also has a marked influence on diminishing substrate inhibition (123).

Drosophila cholinesterase has a single phenylalanine in its acyl pocket; a natural mutation to Y produces a enzyme conferring insecticide resistance to several bulky organophosphates (139).

ACTIVE CENTER-CHOLINE BINDING SUBSITE Four side chains appear to be of particular importance in stabilizing the quaternary moiety of choline. The

crystal structure shows the trimethylammonio-methylene group of decamethonium or the dimethylethylammonio group of edrophonium appears to make a three-point contact with the indole ring of $W_{(84)}$ (84). $F_{(330)}$ and $Y_{(442)}$ are also in close apposition, and some movement of the side chain $F_{(330)}$ towards the aromatic ring of edrophonium is also evident in this complex. The van der Waal's outer shell of the carboxylate of $E_{(199)}$ comes within 1.5Å of that of the trimethylammonio group.

Replacement of $W_{86(84)}$ by A results in a marked reduction in ATCh catalysis and diminished binding of edrophonium (130). A follow-up study shows that the loss of activity is selective for the quaternary substrate since the isosteric, 2,2 dimethylbutyl acetate ester shows little diminution of activity (138). This finding illustrates the importance of the quaternary ammonium-indole interaction in the stabilization of complexes of substrate and inhibitors. However, a large difference in molecular volume is also inherent to this substitution. $W_{(84)}$ is conserved in all the cholinesterases.

The second aromatic residue in this domain is not conserved; the AChEs contain an F or Y at position 337(330) and BuChE has A at 332(330). Several inhibitors selective for BuChE or AChE depend on this difference. The $Y_{337}A$ mutation results in an 10- to 20-fold reduction in edrophonium affinity but little or no reduction in decamethonium affinity (123, 130, 138). By contrast, the affinities of the acridines and particularly certain phenothiazines are increased by this mutation (123). This behavior appears to depend on the phenothiazine side chain and was most marked with ethopropazine where a 2700-fold decrease in K_I was evident. This decrease was virtually identical to its difference in K_I between AChE and BuChE (123). Huperzine shows a decreased affinity with the $Y_{337}A$ substitution (A Saxena, N Qian, IM Kovach, AP Kozikowski, D Vellom, et al, submitted). Taken together, the data indicate that the aromatic group at 337(330) contributes to stabilization of the complexes (i.e. ring stacking and quaternary aromatic interactions in the case of edrophonium and stabilization of the caged structure in the case of huperzine). However, addition of the tricyclic ring system and, in particular, certain substitutions on the exocyclic chain create steric hindrance with the aromatic ring in $F_{(330)}$ or $Y_{(330)}$ This is reflected in lower affinities of inhibitors of larger volume for AChE than for either BuChE or the $Y_{337(330)}A$, AChE mutant (123). The 337(330) residue change has minimal influence on ATCh catalysis. Shafferman and colleagues have shown that the Y_{337} to A mutation diminishes substrate inhibition in human AChE (130) and suggest a direct linkage to the peripheral site. However, upon mutation of Y_{337} to A in mouse AChE substrate inhibition is still evident when examined over a wider range of substrate concentrations (123), which indicates that a substrate inhibition mechanism involving the 337 residue is not universal.

Furthermore, $Y_{(442)}$ also contributes to the choline binding site surface. In BuChE, with $F_{328(330)}$ changed to A, the role of $Y_{440(442)}$ may be more influential. Altered catalytic parameters are found with the $Y_{440}A$ mutation in BuChE (135).

Mutagenesis experiments also revealed that the charge on $E_{(199)}$ stabilizes binding in this region. Edrophonium affinity is markedly reduced (132, 130) and k_{cat}/K_m for ATCh is lowered by a factor of 50 with the $E_{199}Q$ mutation (132). Hence, the energy of stabilization of edrophonium can be partitioned between both the electrostatic and π-electron bonding forces. Similar analyses are possible for other inhibitors, substrates, and transition state mimics. The $E_{199}D$ mutation has less influence on k_{cat}/K_m but markedly affects substrate inhibition (130, 132).

THE PERIPHERAL ANIONIC SITE: GATING AT THE RIM OF THE GORGE Mutagenesis studies reveal that three residues, $W_{286(279)}$, $Y_{72(70)}$ and $Y_{124(121)}$ are critical for dictating specificity of BW284c51, decamethonium, and propidium (123) (Figure 5). These residues are also essential for binding of the peptide, fasciculin (Z Radić, R Duran, DC Vellom, Y Li, C Cervenansky & P Taylor, submitted). Decamethonium and BW284c51 likely span between the choline binding subsite and a portion of the peripheral anionic site whereas propidium and fasciculin are peripheral site selective ligands. In the case of BW284c51 a partitioning of free energy shows essentially linear free energy relationships for summing the contributions of the three residues

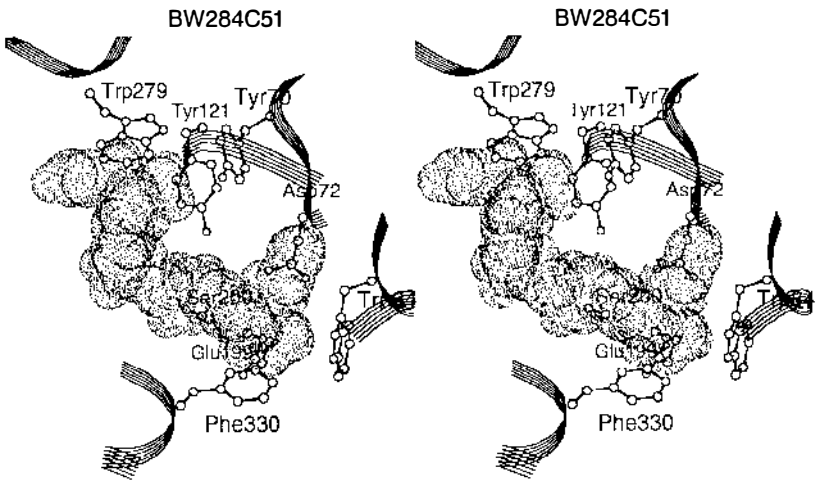

Figure 5 Positions of critical amino acid side chains for an energy minimized complex between BW284c51 and acetylcholinesterase (123).

to stabilization of the complex (123). W_{286} appears to be the most important residue for BW284c51, although each ligand shows slightly different partitioning of free energy. The involvement of only a small number of residues in stabilizing specific complexes is buttressed by the observation that a $BuChE_{1-174}$ $AChE_{175-575}$ chimera behaves like the $Y_{72}N,Y_{124}Q$ mutation and the $Y_{72}N,Y_{124}Q,W_{286}R$ mutation behaves similarly to mouse BuChE for inhibition by BW284c51. This is not the case for decamethonium and propidium, which suggests different binding loci for the latter ligands on the two respective cholinesterases (123).

$D_{74(72)}$ also affects the binding of these ligands (123, 125, 140) and it too is positioned rather close to the rim of the gorge. The site near the rim of the gorge defined by W_{286}, Y_{72}, Y_{124}, D_{74} has several features in common with the W_{86}, F_{337}, Y_{342}, E_{202} site found at the base of the gorge. Since *bis*-quaternary ligands span between the two sites, a similar complement of residues may thus be stabilizing each end of the *bis*-quaternary ligand.

$D_{74(72)}$ is conserved in BuChE as D_{70}. In fact, mutation of this residue to G is responsible for succinylcholine-induced paralysis in man (13, 14, 124, 125); an increased K_m and resistance to dibucaine inhibition and succinylcholine catalysis can be demonstrated in the mutant enzyme (140). Curiously, other mutations that concommitantly appear with the $D_{70}G$, H_{114}, Y_{561} and P_{425} restore some of the catalytic efficiency of the $D_{70}G$ mutation (140). Studies involving a BuChE template and replacement of residues with those found in AChE (135) and BuChE-AChE chimerae (141) have yielded results complementary to those obtained with the AChE template. In *Drosophila*, Y_{109} corresponds to D_{70} and mutations here influence inhibitor specificity (142).

Occupation of the peripheral site affects the conformation of the active center and the configuration of bound ligands at the active center (143, 144). Mutagenesis studies should further delineate the residues involved in this allosteric linkage (123, 138).

The three domains outlined above appear primarily responsible for the reported selectivity of AChE and BuChE for substrates and inhibitors. Specificity for acyl chain length and the propensity for substrate activation or inhibition are governed largely by the two phenylalanines, $F_{295(288)}$ and $F_{297(290)}$, whose side chains outline the acyl pocket. This region also governs the reactivity of isoOMPA for the enzyme; steric hindrance precludes isoOMPA from rapidly reacting with AChE. The BuChE selectivity of ethopropazine arises from its ability to be accommodated in the choline binding subsite. The diethylamino-2-propyl side chain exhibits interference with $F_{337(330)}$ in AChE whereas $A_{332(330)}$ in BuChE enables the fit (123). Finally, the site near the rim of the gorge dictates specificity of the *bis*-quaternary inhibitors and peptides that cannot fit at the base of the gorge; BW284c51, propidium, and fasciculin are the prime examples.

CARBOXYL-TERMINUS Several mutations of this region have emerged from a knowledge of the sequence and alternatively spliced forms. Gibney et al (126) documented the cassette characteristics of the individual exons. By splicing the invariant exons encoding the *Torpedo* enzyme to the exon encoding the glycophospholipid signal (exon 5) through loop-out mutagenesis, the glycophospholipid-linked form of AChE was synthesized in transfected COS cells. By dropping an intermediate exon, a truncated, but inactive, enzyme carrying the glycophospholipid-linkage was formed. By deleting the terminal exons (5 and 6), the expressed enzyme was secreted into thc medium and lacked the glycophospholipid attachment. A natural splice variant in the mouse enzyme yields AChE with the same properties with virtually all of the enzyme appearing in the media (66, 67). Hence, the exon encoding the glycophospholipid linkage signal is both necessary and sufficient for generating the signal sequence for processing and addition of the glycophospholipid. Removal of the cysteine from exon 6 (128) or formation of a truncated hydrophilic form of the enzyme results in secretion of a monomeric enzyme (126). Similar dependencies of membrane attachments have been documented in *Drosophila* cholinesterase (145, 146).

An important development in the study of the assembly process has been the cloning of the gene that encodes the collagen-containing tail species in the *Torpedo* enzyme (147). Although there appear to be multiple tail subunits, coexpression of the cDNA encoding the catalytic subunit and that encoding the tail unit gave rise to the expected asymmetric species for both *Torpedo* and rat catalytic subunit cDNAs (28, 147). Moreover, truncation of thc tail subunit cDNA showed that the amino-terminal portion of the tail molecule contains the sulfhydryl necessary for the intersubunit disulfide linkage (148).

Transfection of the cDNAs encoding the hydrophilic (exon 6) and glycophospholipid-linked (exon 5) forms of AChE generates the expected multiplicity of species seen in vivo (149). Hence, assembly to the various oligomeric species of AChE and processing occur with the transfected cDNAs. Transfection of mouse and human genomic constructs into various cell lines shows tissue selective splicing of mRNA to achieve a diversity of gene products (D Vellom, S Camp, and P Taylor, submitted).

GLYCOSYLATION Human AChE contains three N-linked glycosylation recognition sequences at N_{265}, N_{350}, and N_{464}. Deletion of the recognition sequences singly and in combination diminishes biosynthesis and secretion of the enzyme. The influence appears progressive since an enzyme deficient in all three signals shows the least expression, followed by the mutation with two of the three signals deleted (150). Glycosylation increases the thermal stability of the enzyme, but did not affect the catalytic parameters. Initial studies with the *Drosophila* enzyme also indicate that active enzyme can be synthesized in the absence of glycosylation (146, 151).

CHOLINESTERASE CHIMERAE Construction of cholinesterase chimcrae has been useful in analyzing gene structure in relation to function and in identifying domains of the molecule responsible for particular functional characteristics. The initial approach deleted exon 5 and demonstrated secretion of the *Torpedo* enzyme (126); variants of this construct are discussed above. Attachment of the carboxyl-terminal signal sequence contained in exon 5 to upstream exons or to sequence encoding the amino-terminal portion of the collagen-containing tail unit yielded glycophospholipid-attached enzymes (126, 149). A second approach entailed forming BuChE chimerae between wild-type and naturally occurring mutants (125) and enabled examination of the influcnce of secondary mutations on the $D_{70}G$ mutation (125). Hence, portions of carboxyl-terminal domain of the molecule can modulate the consequences of an amino-terminal modification. Formation of active chimerae between AChE and BuChE have led to assigning domains responsible for inhibitor specificity, for delimiting the selection of residues in site-specific mutagenesis (131, 141). Comparisons of specificity between site-specific mutants and chimerae can often rule out an influence of several residues on inhibitor specificity.

Relationship of Ligand Binding Sites on Acetylcholinesterase to Those on Other Acetylcholine-Binding Proteins

Examination of the high resolution structure of AChE in relation to its functional characteristics and specificity of ligand binding sites may provide insights into the structure of other Ach binding proteins. We have already alluded to the similarities in both the proximal aromatic clusters and the more distant negative charges residing at the choline binding subsite and at the peripheral anionic site in AChE. Further parallels can be drawn with the aromatic clusters in the phosphorylcholine binding antibody and in chemically synthesized host ligands that bind quaternary ligands (87, 88, 152). Chemical labeling studies also show proximity of tyrosines and tryptophan in the vicinity of the ligand binding site on the acetylcholine receptor (153–155). Moreover, tacrine, a ligand that inhibits AChE by binding at the choline subsite (83, 123) also shows a propensity to inhibit K^+-channels. Mutagenesis studies are beginning to define the nature of a quaternary ammonium binding site within the K^+ channel, and a tyrosine substitution for threonine enhances tetraethylammonium inhibition of K^+ conductance (156). However, apart from using proximal aromatic residues and longer range electrostatic forces to stabilize the quaternary ligands and perhaps a more global organization of charges to form a macromolecular dipole to direct the binding of the ligand, there may be few specific parallels between the recognition sites on acetylcholine binding proteins.

In the case of the nicotinic acetylcholine receptor, the ligand binding site appears not to be in the central ion cavity or "gorge"; rather, agonists bind

at distinct sites at the periphery of the receptor (157). Entry of Ach to its two binding sites on the receptor appears to be normal to the axis defined by the ion permeability channel through the membrane. Finally, Ach binding sites are formed at subunit interfaces on the nicotinic receptor rather than being central to one of the subunits.

The muscarinic receptor presents an even different situation since the binding site must be constructed from within the seven membrane-spanning regions (158), a constraint not found for a globular protein or an extracellular domain of a membrane-associated protein.

Ach binds with relatively low affinity to an activatible state of the nicotinic receptor ($K_D \approx 10^{-4}$M), but short-term exposure results in desensitization and concomitant formation of a high-affinity state for Ach, $K_D = 5 \times 10^{-8}$M (153, 159, 160). This low dissociation constant may be contrasted with an AChE K_m of 0.5–1.0 $\times$ 10^{-4}M. Deconstruction of the AChE K_m would indicate that Ach dissociation constant (k_{-1}/k_1 in Scheme 1) is actually larger than K_m. Each state of the nicotinic receptor is designed to recognize the parent ligand whose acetoxy group is planar or trigonal, while in the case of AChE, the site is designed to force the formation of a transition state that is best approximated by a tetrahedral conformation around the carbonyl-containing carbon. The dissociation constant of the enzyme for this transition state, K_{TS}, can be estimated from $K_{TS} = K_m \cdot k_u/k_c$, where k_c/k_u (the ratio of catalyzed and uncatalyzed ester hydrolysis) is the catalytic enhancement provided by the enzyme. The product of K_m ($\sim 10^{-4}$ M) and k_u/k_c ($\sim 10^{-13}$) (113) yields a value of $\sim 10^{-17}$M and reflects a uniquely high affinity for the labile transition state of the substrate. Hence, receptors and AChE are designed to recognize and catalytically force or accommodate distinct conformations of acetylcholine. Accordingly, these unique binding characteristics are likely to be reflected in major differences in molecular and spatial characteristics of their respective binding sites.

Literature Cited

1. Clermont P. 1854. Note sur la préparation de quelques éthers. *CR Acad. Sci. Paris* 39:338–41
2. Argyll-Robinson D. 1863. The calibar bean as a new agent in ophthalmic practice. *Edinburgh Med. J.* 8:815–20
3. Dale HH. 1914. The action of certain esters of choline and their relation to muscarine. *J. Pharmacol. Exp. Ther.* 6:147–90
4. Loewi O, Navratil E. 1926. Über humorale Übertragbarkeit der Herznervenwirkung. XI. Über der Mechanismus der Vaguswirkung von Physostigmin und Ergotamin. *Pfluegers Arch.* 214:689–96
5. Ellman GL, Courtney KD, Andres V

Jr, Featherstone RM. 1961. A new and rapid colorimetric determination of acetylcholinesterase activity. *Biochem. Pharmacol.* 7:88–95

6. Koelle GB, Friedenwald JS. 1949. A histochemical method for localizing cholinesterase activity. *Proc. Soc. Exp. Biol. Med.* 70:617–22
7. Karnovsky MS, Roots L. 1964. A direct coloring thiocholine method for cholinesterase. *J. Histochem. Cytochem.* 12:219–32
8. Taylor P. 1990. Anticholinesterase agents. In *The Pharmacological Basis of Therapeutics*, ed. AG Gilman, LS Goodman, TW Rall, F Murad, AS Nies, P Taylor, pp. 131–49. New York: Pergamon. 8th ed.
9. Schumacher M, Camp S, Maulet Y, Newton M, MacPhee-Quigley K, et al. 1986. Primary structure of *Torpedo californica* acetylcholinesterase deduced from cDNA sequences. *Nature* 319:407–9
10. Sussman JL, Harel M, Frolow F, Oefner C, Goldman A, et al. 1991. Atomic structure of acetylcholinesterase from *Torpedo californica:* a prototypic acetylcholine-binding protein. *Science* 253:872–79
11. Quinn DM. 1987. Acetylcholinesterase: enzyme structure, reaction dynamics, and virtual transition states. *Chem. Rev.* 87:955–79
12. Rosenberry TL. 1975. Acetylcholinesterase. *Adv. Enzymol. Relat. Areas Mol. Biol.* 43:103–218
13. Whittaker M. 1986. Cholinesterases. In *Monographs in Human Genetics*, ed. RS Sparkes, 11:125. Bascl: Karger
14. Soreq H, Zakut H. 1990. Cholinesterase genes: multileveled regulation. In *Monographs in Human Genetics*, ed. RS Sparkes, 13:1–102. Basel: Karger
15. Sussman JL, Silman I. 1992. Acetylcholinesterase: structure and use as a model for specific cation protein interactions. *Curr. Opin. Struct. Biol.* 2:721–29
16. Taylor P. 1991. The cholinesterases. *J. Biol. Chem.* 266:4025–28
17. Massoulié J, Pezzementi L, Bon S, Krejci E, Vallette FM. 1993. Molecular and cellular biology of the cholinesterases. *Prog. Neurobiol.* 41: 31–91
18. Shafferman A, Velan B, eds. 1992. *Multidisciplinary Approaches to Cholinesterase Functions*. New York: Plenum. 293 pp.
19. Swillens S, Ludgate M, Mercken L, Dumont JE, Vassart G. 1986. Analysis of sequence and structure homologies between thyroglobulin and acetylcholinesterase: possible functional and clinical significance. *Biochem. Biophys. Res. Commun.* 137:142–48
20. Hall LMC, Spierer P. 1986. The *Ace* locus of *Drosophila melanogaster:* structural gene for acetylcholinesterase with an unusual 5′ leader. *EMBO J.* 5:2949–54
21. Lockridge O, Bartels CF, Vaughan TA, Wong CK, Norton SE, Johnson LL. 1987. Complete amino acid sequence of human serum cholinesterase. *J. Biol. Chem.* 262:549–57
22. Prody CA, Zevin-Sonkin D, Gnatt A, Goldberg O, Soreq H. 1987. Isolation and characterization of full-length cDNA clones coding for cholinesterase from fetal human tissues. *Proc. Natl. Acad. Sci. USA* 84:3555–59
23. McTiernan C, Adkins S, Chatonnet A, Vaughan TA, Bartels CF, et al. 1987. Brain cDNA clone for human cholinesterase. *Proc. Natl. Acad. Sci. USA* 84:6682–86
24. Rachinsky TL, Camp S, Li Y, Ekström TJ, Newton M, Taylor P. 1990. Molecular cloning of mouse acetylcholinesterase: tissue distribution of alternatively spliced mRNA species. *Neuron* 5:317–27
25. Doctor BP, Chapman TC, Christner CE, Deal CD, De La Hoz DM, et al. 1990. Complete amino acid sequence of fetal bovine serum acetylcholinesterase and its comparison in various regions with other cholinesterases. *FEBS Lett.* 266:123–27
26. Soreq H, Ben-Aziz R, Prody CA, Seidman S, Gnatt A, et al. 1990. Molecular cloning and construction of the coding region for human acetylcholinesterase reveals a G+C-rich attenuating structure. *Proc. Natl. Acad. Sci. USA* 87:9688–92
27. Chatonnet A, Lorca T, Barakat A, Aron E, Jbilo O. 1991. Structure of rabbit butyrylcholinesterase gene deduced from genomic clones and from a cDNA with introns. *Cell Mol. Neurobiol.* 11:119–30
28. Legay C, Bon S, Vernier P, Coussen F, Massoulié J. 1993. Cloning and expression of a rat acetylcholinesterase subunit: generation of multiple molecular forms and complementarity with a *Torpedo* collagenic subunit. *J. Neurochem.* 60:337–46
29. Hall LMC, Malcolm CA. 1991. The acetylcholinesterase gene of *Anopheles stephensi*. *Cell. Mol. Neurobiol.* 11: 131–41
30. Maulet Y, Ballivet M. 1991. Two

different genes encoding cholinesterases in chicken. See Ref. 162, p. 186
31. Rubino S, Mann SKO, Hori RT, Pinko C, Firtel RA. 1989. Molecular analysis of a developmentally regulated gene required for *Dictyostelium* aggregation. *Dev. Biol.* 131:27–36
32. Bomblies L, Biegelmann E, Döring V, Gerisch G, Krafft-Czepa H, et al. 1990. Membrane-enclosed crystals in *Dictyostelium discoideum* cells, consisting of developmentally regulated proteins with sequence similarities to known esterases. *J. Cell Biol.* 110:669–79
33. Oakeshott JG, Collet C, Phillis RW, Nielsen KM, Russell RJ, et al. 1987. Molecular cloning and characterization of esterase-6, a serine hydrolase of *Drosophila*. *Proc. Natl. Acad. Sci. USA* 84:3359–63
34. Collet C, Nielsen KM, Russell RJ, Karl M, Oakeshott JG, Richmond RC. 1990. Molecular analysis of duplicated esterase genes in *Drosophila melanogaster*. *Mol. Biol. Evol.* 7:9–28
35. Mouches C, Pauplin Y, Agarwal M, Lemieux L, Herzog M, et al. 1990. Characterization of amplification core and esterase B1 gene responsible for insecticide resistance in *Culex*. *Proc. Natl. Acad. Sci. USA* 87:2574–78
36. Hanzlik TN, Abdel-Aal YAI, Harshman LG, Hammock BD. 1989. Isolation and sequencing of cDNA clones coding for juvenile hormone esterase from *Heliothis virescens*. Evidence for a catalytic mechanism for the serine carboxylesterases different from that of the serine proteases. *J. Biol. Chem.* 264:12419–25
37. Shimada Y, Sugihara A, Tominaga Y, Izumi T, Tsunasawa S. 1989. cDNA molecular cloning of *Geotrichum candidum* lipase. *J. Biochem.* 106:383–88
38. Long RM, Satoh H, Martin BM, Kimura S, Gonzalez FJ, Pohl LR. 1988. Rat liver carboxylesterase: cDNA cloning, sequencing, and evidence for a multigene family. *Biochem. Biophys. Res. Commun.* 156:866–73
39. Korza G, Ozols J. 1988. Complete covalent structure 60-kDa esterase isolated from 2,3,7,8-tetrachlorodibenzo-p-dioxin-induced rabbit liver microsomes. *J. Biol. Chem.* 263:3486–95
40. Han JH, Stratowa C, Rutter WJ. 1987. Isolation of full-length putative rat lysophospholipase cDNA using improved methods for mRNA isolation and cDNA cloning. *Biochemistry* 26: 1617–25
41. Kyger EM, Wiegand RC, Lange LG. 1989. Cloning of the bovine pancreatic cholesterol esterase/lysophospholipase. *Biochem. Biophys. Res. Commun.* 164: 1302–9
42. Ollis DL, Cheah E, Cygler M, Dijkstra B, Frolow F, et al. 1992. The α/β hydrolase fold. *Prot. Eng.* 5:197–211
43. Cooper A, Russey H. 1989. Characterization of the yeast KEX1 gene product: a carboxypeptidase involved in processing secreted precursor proteins. *Mol. Cell. Biol.* 9:2706–14
44. Franken SM, Rozeboom HJ, Kalk KH, Dijkstra BW. 1991. Crystal structure of haloalkane dehalogenase: an enzyme to detoxify halogenated alkanes. *EMBO J.* 10:1297–302
45. Pathak D, Ngai KL, Ollis D. 1988. X-ray crystallographic structure of dienelactone hydrolase at 2.8 Å. *J. Mol. Biol.* 204:435–45
46. Olson PF, Fessler LI, Nelson RE, Campbell AG, Fessler JH. 1990. Glutactin, a novel *Drosophila* basement membrane related glycoprotein with sequence similarity to serine esterases. *EMBO J.* 9:3593–601
47. De la Escalera S, Backamp E-O, Moya F, Piovant M, Jimenez F. 1990. Characterization and gene cloning of neurotactin, a *Drosophila* transmembrane protein related to cholinesterases. *EMBO J.* 9:3593–601
48. Gentry MK, Doctor BP. 1991. Alignment of amino acid sequences of acetylcholinesterases and butyrylcholinesterases. See Ref. 162, pp. 394–98
49. Cygler M, Schrag J, Sussman JL, Harel M, Silman I, et al. 1993. Relationship between sequence conservation and three-dimensional structure in a large family of esterases, lipases, and related proteins. *Protein Sci.* 2: 366–82
50. MacPhee-Quigley K, Vedvick TS, Taylor P, Taylor SS. 1986. Profile of disulfide bonds in acetylcholinesterase. *J. Biol. Chem.* 261:13565–70
51. Lockridge O, Adkins S, La Du BN. 1987. Location of disulfide bonds within the sequence of human serum cholinesterase. *J. Biol. Chem.* 262: 12945–52
52. MacPhee-Quigley K, Taylor P, Taylor SS. 1985. Primary structures of the catalytic subunits from two molecular forms of acetylcholinesterase: a comparison of NH2-terminal and active center sequences. *J. Biol. Chem.* 260: 12185–89
53. Gibney G, Camp S, Dionne M, MacPhee-Quigley K, Taylor P. 1990. Mu-

tagenesis of essential functional residues in acetylcholinesterase. *Proc. Natl. Acad. Sci. USA* 87:7546–50
54. Augustinsson KB. 1948. Cholinesterases: a study in comparative enzymology. *Acta Physiol. Scand.* 15 (Suppl. 52:1–182
55. Silver A. 1974. *The Biology of Cholinesterases*. Amsterdam: North-Holland
56. Gnagey AL, Forte M, Rosenberry TL. 1987. Isolation and characterization of acetylcholinesterase from *Drosophila*. *J. Biol. Chem.* 262:1140–45
57. Toutant J-P, Massoulié J, Bon S. 1985. Polymorphism of pseudocholinesterase in *Torpedo marmorata* tissues: comparative study of the catalytic and molecular properties of this enzyme with acetylcholinesterase. *J. Neurochem.* 44:580–92
58. Johnson CD, Rand JB, Herman RK, Stern BD, Russell RL. 1988. The acetylcholinesterase genes of *C. elegans:* identification of a third gene (ace-3) and mosaic mapping of a synthetic lethal phenotype. *Neuron* 1:165–73
59. Arpagaus M, Richier P, L'Hermitte Y, Le Roy F, Bergé J, et al. 1992. Nematode acetylcholinesterases: several genes and molecular forms of their products. See Ref. 18, pp. 65–74
60. Maulet Y, Camp S, Gibney G, Rachinsky TL, Ekström TJ, Taylor P. 1990. A single gene encodes glycophospholipid-anchored and asymmetric acetylcholinesterase forms: alternative coding exons contain inverted repeat sequences. *Neuron* 4:289–301
61. Li Y, Camp S, Rachinsky TL, Getman DK, Taylor P. 1991. Gene structure of mammalian acetylcholinesterase: alternative exons dictate tissue-specific expression. *J. Biol. Chem.* 266:23083–90
62. Arpagaus M, Kott M, Vatsis KP, Bartels CF, La Du BN, Lockridge O. 1990. Structure of the gene for human butyrylcholinesterase. Evidence for a single copy. *Biochemistry* 29:124–31
63. Sikorav JL, Krejci E, Massoulié J. 1987. cDNA sequences of *Torpedo marmorata* acetylcholinesterase: primary structure of the precursor of a catalytic subunit; existence of multiple 5′-untranslated regions. *EMBO J.* 6: 1865–73
64. Sikorav JL, Duval N, Anselmet A, Bon S, Krejci E, et al. 1988. Complex alternative splicing of acetylcholinesterase transcript in *Torpedo* electric organ; primary structure of the precursor of the glycolipid-anchored dimeric form. *EMBO J.* 7:2983–93
65. Schumacher M, Maulet Y, Camp S, Taylor P. 1988. Multiple messenger RNA species give rise to the structural diversity in acetylcholinesterase. *J. Biol. Chem.* 263:18979–87
66. Li Y, Camp S, Taylor P. 1993. Tissue-specific expression and alternative mRNA processing of the mammalian acetylcholinesterase gene. *J. Biol. Chem.* 268:5790–97
67. Li Y, Camp S, Rachinsky TL, Bongiorno C, Taylor P. 1993. Promoter elements and transcriptional control of the mouse acetylcholinesterase gene. *J. Biol. Chem.* 268:3563–72
68. Gibney G, MacPhee-Quigley K, Thompson B, Vedvick T, Low MG, et al. 1988. Divergence in primary structure between molecular forms of acetylcholinesterase. *J. Biol. Chem.* 263:1140–45
69. Rotundo RL, Gomez AM, Fernandez-Valle C, Randall WR. 1988. Allelic variants of acetylcholinesterase forms in avian nerves and muscle and encoded by a single gene. *Proc. Natl. Acad. Sci. USA* 52:7121–25
70. Getman DK, Eubanks J, Evans G, Taylor P. 1992. Assignment of the human acetylcholinesterase gene to chromosome 7q22. *Am. J. Hum. Genet.* 50:170–77
71. Ehrlich G, Viegas-Pequignot E, Ginzberg D, Sindel L, Soreq H, Zakut H. 1992. Mapping the human acetylcholinesterase gene to chromosome 7q22 by fluorescent *in situ* hybridization coupled with selective PCR amplification from a somatic hybrid cell panel and chromosome-sorted DNA libraries. *Genomics* 13:1192–97
72. Gaughan G, Park H, Priddle J, Craig I, Craig S. 1991. Refinement of the localization of human butyrylcholinesterase to chromosome 3q26.1-q26.2 using a PCR-derived probe. *Genomics* 11:455–58
73. Allderdice PW, Gardner HAR, Galutira D, Lockridge O, La Du BN, McAlpine PJ. 1991. The cloned butyrylcholinesterase (*BCHE*) gene maps to a single chromosome site, 3q26. *Genomics* 11:452–54
74. Rachinsky TL, Crenshaw EB III, Taylor P. 1992. Assignment of the gene for acetylcholinesterase to distal mouse-chromosome 5. *Genomics* 14:511–14
75. Sussman JL, Harel M, Frolow F, Varon L, Toker L, et al. 1988. Purification and crystallization of a dimeric form of acetylcholinesterase from *Torpedo*

californica subsequent to solubilization with phosphatidylinositol-specific phospholipase. *J. Mol. Biol.* 203:821–23
76. Schrag JD, Schmid MF, Morgan DG, Phillips GN, Wah C, Tang L. 1988. Crystallization and preliminary X-ray diffraction analysis of 11S acetylcholinesterase. *J. Biol. Chem.* 263: 9795–801
77. Schrag JD, Li Y, Wu S, Cygler M. 1991. Ser-His-Glu triad forms the catalytic site of the lipase from *Geotrichum candidum*. *Nature* 351: 761–64
78. Harel M, Sussman JL, Krejci E, Bon S, Chanal P, et al. 1992. Conversion of acetylcholinesterase to butyrylcholinesterase, modeling and mutagenesis. *Proc. Natl. Acad. Sci. USA* 89: 10827–31
79. Rosenberry TL, Neumann E. 1977. Interaction of ligands with acetylcholinesterase. Use of temperature-jump relaxation kinetics in the binding of specific fluorescent ligands. *Biochemistry* 16:3870–78
80. Nolte HJ, Rosenberry TL, Neumann E. 1980. Effective charge on acetylcholinesterase active sites determined from the ionic strength dependence of association rate constants with cationic ligands. *Biochemistry* 19:3705–11
81. Tan RC, Truong TN, McCammon JA, Sussman JL. 1993. Acetylcholinesterase: electrostatic steering increases the rate of ligand binding. *Biochemistry* 32:401–3
82. Ripoll DR, Faerman CH, Axelsen PH, Silman I, Sussman JL. 1993. An electrostatic mechanism for substrate guidance down the aromatic gorge of acetylcholinesterase. *Proc. Natl. Acad. Sci. USA* 90:5128–32
83. Sussman JL, Harel M, Silman I. 1992. Three dimensional structure of acetylcholinesterase. See Ref. 18, pp. 95–108
84. Harel M, Schalk I, Ehret-Sabatier L, Bouet F, Goeldner M, et al. 1993. Quaternary ligand binding site of acetylcholinesterase as revealed by X-ray crystallography and photoaffinity labelling. *Proc. Natl. Acad. Sci. USA*. 90:9031–35
85. Hasan FB, Cohen SG, Cohen JB. 1980. Hydrolysis by acetylcholinesterase. Apparent molal volumes and trimethyl and methyl subsites. *J. Biol. Chem.* 255:3898–904
86. Cohen SG, Salih E, Solomon M, Howard S, Chishti SB, Cohen JB. 1989. Reactions of 1-bromo-2-[^{14}C]pinacolone with acetylcholinesterase from *Torpedo nobiliana*. Effects of 5-trimethylammonio-2-pentanone and diisopropyl fluorophosphate. *Biochem. Biophys. Acta* 997:167–75
87. Dougherty DA, Stauffer DA. 1990. Acetylcholine binding by a synthetic receptor: implication for biological recognition. *Science* 250:1558–60
88. Segal DM, Padlan EA, Cohen GH, Rudikoff S, Potter M, Davies DR. 1974. The three-dimensional structure of phosphorylcholine—binding mouse immunoglobulin Fab and the nature of the antigen binding site. *Proc. Natl. Acad. Sci. USA* 71:4295–302
89. Pressman D, Grossberg AL, Pence LH, Pauling L. 1946. The reaction of antiserum homologous to the p-azo phenyltrimethylammonium group. *J. Am. Chem. Soc.* 68:250–55
90. Changeux J-P. 1966. Responses of acetylcholinesterase from *Torpedo marmorata* to salts and curarizing drugs. *Mol. Pharmacol.* 2:369–92
91. Taylor P, Lappi S. 1975. Interaction of fluorescence probes with acetylcholinesterase. The site and specificity of propidium binding. *Biochemistry* 14: 1989–97
92. Berman HA, Yguerabide J, Taylor P. 1980. Fluorescence energy transfer on acetylcholinesterase: spatial relationship between peripheral site and active center. *Biochemistry* 19:2226–35
93. Weise C, Kreienkamp HJ, Raba R, Pedak A, Aaviksaar A, Hucho F. 1990. Anionic subsites of the acetylcholinesterase from *Torpedo californica:* affinity labelling with the cationic reagent *N,N*-dimethyl-2-phenyl-aziridinium. *EMBO J.* 9:3885–88
94. Amitai G, Taylor P. 1991. Characterization of peripheral anionic site peptides of AChE by photoaffinity labeling with monoazidopropidium (MAP). See Ref. 162, p. 285
95. Haas R, Adams EW, Rosenberry MA, Rosenberry TL. 1992. Substrate-selective inhibition and peripheral site labeling of acetylcholinesterase by platinum(terpyridine)chloride. See Ref. 18, pp. 131–40
96. Marchot P, Khelif A, Ji YH, Mansuelle P, Bougis PE. 1993. Binding of ^{125}I-fasciculin to rat brain acetylcholinesterase. The complex still binds diisopropyl fluorophosphate. *J. Biol. Chem.* 268:12458–67
97. Cervenansky C, Dajas F, Harvey AL, Karlsson E. 1991. The fasciculins. In *Snake Toxins,* ed. AC Harvey, pp. 303–21. New York: Pergamon
98. Radić Z, Reiner E, Taylor P. 1991.

Role of the peripheral anionic site on acetylcholinesterase: inhibition by substrates and coumarin derivatives. *Mol. Pharmacol.* 39:98–104

99. Berman HA, Nowak MW. 1992. Influence of ion composition of the medium on acetylcholinesterase conformation. See Ref. 18, pp. 149–56
100. Wilson IB, Quan C. 1958. Acetylcholinesterase studies on molecular complementariness. *Arch. Biochem. Biophys.* 73:131–38
101. Kreienkamp HJ, Weise C, Raba R, Aaviksaar A, Hucho F. 1991. Anionic subsites of the catalytic center of acetylcholinesterase from *Torpedo* and from cobra venom. *Proc. Natl. Acad. Sci. USA* 88:6117–21
102. Schalk I, Ehret-Sabatier L, Bouet F, Goeldner M, Hirth C. 1992. Structural analysis of acetylcholinesterase ammonium binding sites. See Ref. 18, pp. 117–20
103. Shinitzky M, Dudai Y, Silman I. 1973. Spectral evidence for the presence of tryptophan in the binding site of acetylcholinesterase. *FEBS Lett.* 30: 125–28
104. Mooser G, Sigman DS. 1974. Ligand binding properties of acetylcholinesterase determined with fluorescent probes. *Biochemistry* 13:2299–307
105. Barnett P, Rosenberry TL. 1977. Catalysis by acetylcholinesterase: acceleration of the hydrolysis of neutral acetic acid esters by certain aromatic cations. *J. Biol. Chem.* 252:7200–6
106. Berman HA, Leonard K. 1989. Chiral reactions of acetylcholinesterase probed with enantiomeric methylphosphonothioates. Noncovalent determinants of enzyme chirality. *J. Biol. Chem.* 264:3942–50
107. Belleau B, DiTullio V. 1970. Kinetic effects of alkyl quaternary ammonium salts on the methanesulfonylation of the acetylcholinesterase catalytic center. Significance of substituent volumes and binding enthalpies. *J. Am. Chem. Soc.* 92:6320–25
108. Belleau B, DiTullio V, Tsai Y-H. 1970. Kinetic effects of leptocurares and pachycurares on the methanesulfonylation of acetylcholinesterase. A correlation with pharmacodynamic properties. *Mol. Pharmacol.* 6:41–45
109. Wilson IB. 1967. Conformation changes in acetylcholinesterase. *Ann. NY Acad. Sci.* 144:664–79
110. Taylor P, Jacobs NM. 1974. Interaction between bisquaternary ammonium ligands and acetylcholinesterase: complex formation studied by fluorescence quenching. *Mol. Pharmacol.* 10:93–107
111. Wee VT, Sinha BK, Taylor P, Chignell CF. 1976. Interaction of spin-labeled bisquaternary ammonium ligands with acetylcholinesterase. *Mol. Pharmacol.* 12:667–77
112. Aldridge WN, Reiner E. 1972. *Enzyme Inhibitors as Substrates,* Amsterdam: Elsevier. 328 pp.

112a. Himel CM, Taylor JL, Pape C, Millar DB, Christopher J, Kurlansik L. 1979. Acridine araphanes: a new class of probe materials for biological receptors. *Science* 205:1277–79

113. Bazclyansky M, Robey E, Kirsch JF. 1986. Fractional diffusion limited component of reactions catalyzed by acetylcholinesterase. *Biochemistry* 25: 125–32
114. Quinn DM, Pryor AN, Selwood T, Lee BH, Acheson SA, Barlow PN. 1991. The chemical mechanism of acetylcholinesterase reactions. Biological catalysis at the speed limit. See Ref. 162, pp. 252–57
115. Froede HC, Wilson IB. 1984. Direct determination of acetyl-enzyme intermediate in the acetylcholinesterase catalysis of acetylcholine and acetylthiocholine. *J. Biol. Chem.* 259:11010–13
116. Quinn DM, Selwood T, Pryor AN, Lee BH, Leu L-S, et al. 1992. Cryptic catalysis and cholinesterase function. See Ref. 18, pp. 141–48
117. Albery WJ, Knowles JR. 1976. Evolution of enzyme function and the development of catalytic efficiency. *Biochemistry* 15:5631–40
118. Rosenberry TL. 1975. Catalysis by acetylcholinesterase: Evidence that the rate-limiting step for acylation with certain substrates precedes general acid-base catalysis. *Proc. Natl. Acad. Sci. USA* 72:3834–38
119. Pryor AN, Selwood T, Leu L-S, Andracki MA, Lee BH, et al. 1992. Simple general acid-base catalysis of physiological acetylcholinesterase reactions. *J. Am. Chem. Soc.* 114:3896–900
120. Krupka RM, Laidler KJ. 1961. Molecular mechanisms for hydrolytic enzyme action II. Inhibition of acetylcholinesterase by excess substrate. *J. Am. Chem. Soc.* 83:1448–54
121. Augustinsson KB, Bartfai T, Mancrvik B. 1974. A steady state model for butyrylcholinesterase from horse plasma. *Biochem. J.* 141:825–34
122. Cauet G, Friboulet A, Thomas D. 1987. Horse serum butyrylcho-

linesterase kinetics: a molecular mechanism based on inhibition studies with dansylaminoethyl trimethylammonium. *Biochem. Cell. Biol.* 65:529–35

123. Radic Z, Pickering N, Vellom DC, Camp S, Taylor P. 1993. Three distinct domains in the cholinesterase molecule confer selectivity for acetylcholinesterase and butyrylcholinesterase inhibitors. *Biochemistry*. 32:12074–84
124. La Du BN, Bartels CF, Nogueira CP, Arpagaus M, Lockridge O. 1991. Proposed nomenclature for human butyrylcholinesterase genetic variants identified by DNA sequencing. *Cell. Mol. Neurobiol.* 11:79–90
125. Neville LF, Gnatt A, Padan R, Seidman S, Soreq H. 1990. Anionic site interactions in human butyrylcholinesterase disrupted by two single point mutations. *J. Biol. Chem.* 265: 20735–38
126. Gibney G, Taylor P. 1990. Biosynthesis of *Torpedo* acetylcholinesterase in mammalian cells. Functional expression and mutagenesis of the glycophospholipid-anchored form. *J. Biol. Chem.* 265:12576–83
127. Soreq H, Seidman S. 1992. *Xenopus* oocyte microinjection: from gene to protein. *Methods Enzymol.* 207:225–65
128. Velan B, Grosfeld H, Kronman C, Leitner M, Gozes Y. 1991. The effect of elimination of intersubunit disulfide bonds on the activity, assembly, and secretion of recombinant human acetylcholinesterase: expression of acetylcholinesterase CYS-580-Ala mutant. *J. Biol. Chem.* 266: 23977–84
129. Shafferman A, Kronman C, Flashner Y, Leitner M, Grosfeld H, et al. 1992. Mutagenesis of human acetylcholinesterase; identification of residues involved in catalytic activity and in polypeptide folding. *J. Biol. Chem.* 267:17640–48
130. Shafferman A, Velan B, Ordentlich A, Kronman C, Grosfeld H, et al. 1992. Substrate inhibition of acetylcholinesterase: residues involved in signal transduction from the surface to the catalytic center. *EMBO J.* 11: 3561–68
131. Vellom DC, Radic Z, Li Y, Pickering NA, Camp S, Taylor P. 1993. Amino acid residues controlling acetylcholinesterase and butyrylcholinesterase specificity. *Biochemistry* 32:12–17
132. Radic Z, Gibney G, Kawamoto S, MacPhee-Quigley K, Bongiorno C, Taylor P. 1992. Expression of recombinant acetylcholinesterase in a *Baculovirus* system: kinetic properties of glutamate 199 mutants. *Biochemistry* 31:9760–67
133. Fischer M, Ittah A, Liefer I, Gorecki M. 1993. Expression and recognition of biologically active human acetylcholinesterase from *E. coli*. *Cell Mol. Neurobiol.* 13:25–38
134. Duval N, Bon S, Silman I, Sussman JL, Massoulié J. 1992. Site-directed mutagenesis of active site-related residues in *Torpedo* acctylcholinesterase. Presence of a glutamic acid in the catalytic triad. *FEBS Lett.* 309:421–23
135. Gnatt A, Lowenstein Y, Yaron A, Schwarz M, Soreq H. 1993. Site-directed mutagenesis of active site residues reveals plasticity of human butyrylcholinesterase in substrate and inhibitor interactions. *J. Neurochem.* In press
136. Krejci E, Duval N, Chatonnet A, Vincens P, Massoulié J. 1991. Cholinesterase-like domains in enzymes and structural proteins: functional and evolutionary relationships and identification of a catalytically essential aspartic acid. *Proc. Natl. Acad. Sci. USA* 88:6647–51
137. Chatel JM, Grassi J, Frobert Y, Massoulié J, Vallette FM. 1993. Existence of an inactive pool of acetylcholinesterase in chicken brain. *Proc. Natl. Acad. Sci. USA* 90:2476–80
138. Ordentlich A, Barak D, Kronman C, Flashner Y, Leitner M, et al. 1993. Dissection of the human acetylcholinesterase active center—Determinants of substrate specificity. *J. Biol. Chem.* 268:17083–95
139. Fournier D, Bride J-M, Hoffmann F, Karch F. 1992. Acetylcholinesterase: two types of modifications confer resistance to insecticide. *J. Biol. Chem.* 267:14270–74
140. Neville LF, Gnatt A, Loewenstein Y, Seidman S, Ehrlich G, Soreq H. 1992. Intramolecular relationships in cholinesterases revealed by oocyte expression of site-directed and natural variants of human BCHE. *EMBO J.* 11:1641–49
141. Lowenstein Y, Gnatt A, Neville LF, Soreq H. 1993. A chimeric human cholinesterase: identification of interaction sites responsible for recognition of acetyl-, butyrylcholinesterase specific ligands. *J. Mol. Biol.* 234:289–96
142. Mutero A, Pravalorio M, Simeon V, Fournier D. 1992. Catalytic properties

of cholinesterases: importance of tyrosine 109 in *Drosophila* protein. *NeuroReport* 3:39–42

143. Epstein DJ, Berman HA, Taylor P. 1979. Ligand-induced conformational changes in acetylcholinesterase investigated with fluorescent phosphonates. *Biochemistry* 18:4749–54
144. Berman HA, Becktel W, Taylor P. 1981. Spectroscopic studies on acetylcholinesterase: influence of peripheral-site occupation on active-center conformation. *Biochemistry* 20: 4803–10
145. Fournier D, Mutero A, Rungger D. 1992. *Drosophila* acetylcholinesterase: expression of a functional precursor in *Xenopus* oocytes. *Eur. J. Biochem.* 203:513–19
146. Fournier D, Mutero A, Pravalorio M, Bride J-M. 1992. *Drosophila* acetylcholinesterase: analysis of structure and sensitivity to insecticides by in vitro mutagenesis and expression. See Ref. 18, pp. 75–82
147. Krejci E, Coussen F, Duval N, Chatel JM, Legay C, et al. 1991. Primary structure of a collagenic tail subunit of *Torpedo* acetycholinesterase: co-expression with catalytic subunit induces the production of collagen-tailed forms in transfected cells. *EMBO J.* 10:1285–93
148. Duval N, Krejci E, Grassi J, Coussen F, Massoulié J, Bon S. 1992. Molecular architecture of acetylcholinesterase collagen-tailed forms; construction of a glycolipid-tailed tetramer. *EMBO J.* 9:3255–61
149. Duval N, Massoulié J, Bon S. 1992. H and T subunits of acetylcholinesterase from *Torpedo*, expressed in COS cells, generate all types of globular forms. *J. Cell Biol.* 118:641–53
150. Velan B, Kronman C, Ordentlich A, Flashner Y, Leitner M, et al. 1993. N-glycosylation of human acetylcholinesterase effects enzyme stability and secretion efficiency but not enzymatic activity. *Biochem. J.* In press
151. Mutero A, Fournier D. 1992. Post-translational modifications of *Drosophila* acetylcholinesterase. In vitro mutagenesis and expression in *Xenopus* oocytes. *J. Biol. Chem.* 267: 1695–700
152. McCury A, Jimenez L, Stauffer DA, Dougherty DA. 1992. Biomimetic catalysis of S_N2 reactions through cation-π interactions. The role of polarizability in catalysis. *J. Am. Chem. Soc.* 114:10314–21
153. Changeux J-P, Galzi J-L, Devillers-Thiery A, Bertrand D. 1992. The functional architecture of the acetylcholine nicotinic receptor explored by affinity labelling and site-directed mutagenesis. *Q. Rev. Biophys.* 25:395–432
154. Abramson SN, Li Y, Culver P, Taylor P. 1989. An analog of lophotoxin reacts covalently with Tyr^{190} in the α-subunit of the nicotinic acetylcholine receptor. *J. Biol. Chem.* 264:12666–72
155. Cohen JB, Sharp SD, Liu WS. 1991. Structure of the agonist-binding site of the nicotinic acetylcholine receptor: [^{3}H]acetylcholine mustard identifies residues in the cation-binding subsite. *J. Biol. Chem.* 266:23354–64
156. Heginbotham L, MacKinnon R. 1992. The aromatic binding site for tetraethylammonium ion on potassium channels. *Neuron* 8:483–91
157. Unwin NJM. 1993. Nicotinic acetylcholine receptor at 9 Å resolution. *J. Mol. Biol.* 229:1101–24
158. Hulme EC, Kurtenbach E, Curtis CA. 1991. Muscarinic acetylcholine receptors: structure and function. *Biochem. Soc. Trans.* 19:133–38
159. Taylor P, Johnson DA, Brown RD. 1983. The linkage between ligand occupation and response of the nicotinic acetylcholine receptor. In *Advances in Membranes and Transport*, ed. A Kleinzeller, BR Martin, pp. 407–43. New York: Academic
160. Sine SM, Claudio T, Sigworth FJ. 1990. Activation of *Torpedo* acetylcholine receptors in mouse fibroblasts: Single channel current kinetics reveal distinct agonist binding affinities. *J. Gen. Physiol.* 153:305–12
161. Bartels CF, Zelinski T, Lockridge O. 1993. Mutation at codon 322 in the human acetylcholinesterase (ACHE) gene accounts for YT blood group polymorphism. *Am. J. Hum. Genet.* 52:928–36
162. Massoulié J, Bacou F, Barnard E, Chatonnet A, Doctor BP, Quinn DM, eds. 1991. *Cholinesterases: Structure, Function, Mechansism, Genetics and Cell Biology*. Washington, DC: Am. Chem. Soc. 414 pp.
163. Mason P, Adkins S, Gouet P, Lockridge O. 1993. Recombinant human butyrylcholinesterase G390V, the fluoride-2 variant expressed in Chinese hamster ovary cells, is a low affinity variant. *J. Biol. Chem.* 268:14329–41
164. Fournier D, Mutero A, Pravalorio M,

Bride JM. 1993. *Drosophila* acetylcholinesterase: mechanism of resistance to organophosphates. *Chem. Biol. Interact.* 87:233–38

165. Kerem A, Kronman C, Bar-Nun S, Shafferman A, Velan B. 1993. Interrelations between assembly and secretion of recombinant human acetylcholinesterase. *J. Biol. Chem.* 268: 180–84
166. Saxena A, Doctor BP, Maxwell DM, Lenz DE. Radicac Z, Taylor P. 1993. The role of glutamate 199 in the aging of cholinesterase. *Biochem. Biophys. Res. Commun.* In Press